Supporting information

Biosynthesis of Cyclohexanecarboxyl-CoA Highlights a Promiscuous Shikimoyl-CoA Synthetase and a FAD-dependent Dehydratase

Will Skyrud[1], Antonio Del Rio Flores[2], Wenjun Zhang[2,3*]

[1]Department of Chemistry, [2]Department of Chemical and Biomolecular Engineering, University of California, Berkeley, California 94720, United States

[3]Chan Zuckerberg Biohub, San Francisco, CA 94158, United States

***E-mail correspondence:**
wjzhang@berkeley.edu

Experimental Methods

Tables

Figures

References

Experimental Methods

Growth media, strains and reagents. The DNA constructs and bacterial strains used in this study are listed in **Table S1 and S2**, respectively. Chemicals and media were purchased from Fisher Scientific or Sigma-Aldrich unless otherwise stated. Phusion High-Fidelity PCR Master Mix (NEB) was used for PCR reactions. Restriction and ligation enzymes were purchased from Thermo Scientific and New England Biolabs, respectively, unless otherwise stated.

Construction of plasmids for protein expression in *E. coli.* Individual genes were PCR amplified from cosmid or genomic DNA. All primers are listed in **Table S3**. Gibson assembly was used to ligate PCR products to linear pET30. Plasmids were isolated using a Zyppy Miniprep Kit (Zymo Research) and confirmed by DNA sequencing (UC Berkeley DNA Sequencing Facility). The N- and C-terminal of *asuB1, asuB1*$_C$ and *asuB1*$_N$, respectively, as well as *asuB3* were amplified from the pART1361 cosmid[1]. The *asuB2* gene was cloned from two separate sources to result in the purification of the apo and holo form. The apo form of AsuB2 that was used to determine the FAD dependence of B2 catalyzed dehydration resulted from expression of *asuB2* from the pART1361 cosmid. The holo form of AsuB2 that was used in all other biochemical assays and protein characterization was an *asuB2* homolog amplified from *L. aerocolonigenes* genomic DNA.

Overproduction and Purification of Recombinant Protein. Expression strains were grown in 0.7 L of LB supplemented with 50 μg/mL of kanamycin or 1.0 L of Terrific Broth (TB) with 50 μg/mL of kanamycin at 37 °C and 250 rpm until an OD_{600} of 0.5. Cultures were then cooled on ice for 10 minutes before induction with 120 μM IPTG. Induction of gene expression lasted for 16 h at 16 °C and 200 rpm. The cells were then harvested by centrifugation (6000 x g, 15 min, 4 °C), and supernatant was removed. The pellet was resuspended in 30 mL of lysis buffer (25 mM HEPES, pH 8, 0.5 M NaCl, 5 mM imidazole) and homogenized using an Avestin homogenizer. The insoluble fraction was removed by centrifugation (15,000 rpm, 1 h, 4 °C), and the supernatant was filtered with a 0.45 μM filter before batch binding. Ni-NTA resin (Qiagen) was added to the filtrate at 2 mL/L of cell culture, and samples were allowed to nutate for 1 hour at 4 °C. The protein resin mixture was added to a gravity filter column. The flow through was discarded, the column was then washed with approximately 24 mL of wash buffer (25 mM HEPES, 300 mM NaCl, pH 8) and tagged protein was eluted in approximately 18 mL of elution buffer (25 mM HEPES, 100 mM NaCl, 250 mM imidazole, pH 8). Complete elution was determined by Bradford assay. Purified proteins were then concentrated and exchanged into appropriate buffer (25 mM HEPES, 100 mM NaCl, pH 8) using Amicon ultra filter units. After two rounds of exchange and concentration, pure protein was removed, and glycerol was added to a final concentration of 8%. Proteins were flash frozen in liquid nitrogen and stored at −80 °C or used immediately for in vitro assays. Presence and purity of enzymes was assessed using SDS-page and concentration was determined using a NanoDrop UV-Vis spectrophotometer (Thermo Fisher). The approximate protein yields were 21 mg/L for AsuB1$_C$ (65 kDa), 34 mg/L for AsuB2 (*L. aerocolonigenes*, 48 kDa), 22 mg/L for AsuB2 (*S. asukabaensis,* 48 kDa), and 48 mg/L for AsuB3 (34 kDa). Notably, AsuB2 from *L. aerocolonigenes* purified as a holo protein with an obvious yellow color. Due to this it was used in all biochemical and cofactor determination assays. AsuB2 from *S. asukabaensis* purified without yellow color and was assumed to be the apo protein. This protein was therefore used to determine the FAD dependence of AsuB2 and proved to be the apo form as purified.

Enzymatic Synthesis of Acyl-CoAs by AsuB1$_C$. Reactions were performed at room temperature for one hour in 50 µL of 25 mM ammonium bicarbonate (pH 7.5) containing 1mM $MgCl_2$, 1 mM ATP, 1 mM CoA, 2 mM acid substrate and 20 µM AsuB1$_C$. Acid substrates were suspended in methanol to aid in solubility and added to reactions at 2% total volume. Reactions were quenched by the addition of an equal volume of 10% trifluoroacetic acid (TFA), precipitated protein was removed by centrifugation (10,000 x g, 2 min) and the supernatant was used for analysis. LC-UV-MS analysis was performed on an Agilent 6120 single quadrupole LC/MS equipped with an Agilent Eclipse Plus C18 column (4.6 x 100 mm). A linear gradient of 10-50% CH_3CN with 0.1% formic acid (v/v) over 40 minutes in H_2O with 0.1% formic acid (v/v) with a flow rate of 0.5 mL/min was used. In the case of shikimate, the same criteria as above were used, but the gradient was adjusted to 2-10% over 20 minutes to allow separation of CoA and shikimoyl-CoA. In all cases the fragmentor voltage was decreased to 50 V to aid in detection of CoA ligated products and absorbance was monitored at 260 nm.

ATP-PP$_i$ Release Assays for Kinetic Investigation of AsuB1$_C$. The inorganic pyrophosphate released by enzymatic reaction was measured continuously using the EnzChek Pyrophosphate Assay Kit (Thermo Fisher). A typical assay contained, in a total volume of 100 µL, 0-10 mM acid substrate, 1mM ATP, 2 mM $MgCl_2$, 1 mM CoA, 1 µM AsuB1$_C$. The 20x reaction buffer, MESG substrate, purine nucleoside phosphorylase and inorganic pyrophosphatase were added according to the protocol. Reactions were initiated by the addition of the acid substrate and monitored at 360 nm. Initial velocities were calculated using the standard curve for inorganic pyrophosphate. The data were fitted to the Michaelis-Menten equation in GraphPad Prism to obtain estimates for k_{cat} and K_m.

Enzymatic reduction of Acyl-CoAs by AsuB3. Coupled enzymatic reactions were performed at room temperature for two hours in 50 µL of 50 mM TRIS (pH 7.5) containing 1mM $MgCl_2$, 1 mM ATP, 1 mM CoA, 2 mM acid substrate, 20 µM AsuB1$_C$, with and without 20 µM AsuB3 and 4 mM NADPH. Reactions were quenched with an equal volume of 10% TFA, precipitated protein was removed by centrifugation (10,000 x g, 2 min) and the supernatant was used for analysis. LC-HRMS analysis was performed on an Agilent technologies 6545 Accurate-Mass Q-TOF LC-MS instrument with an Agilent Eclipse Plus C18 column (4.6 x 100 mm). A linear gradient of 10-35% CH_3CN with 0.1% formic acid (v/v) over 30 minutes in H_2O with 0.1% formic acid (v/v) with a flow rate of 0.5 mL/min was used. The fragmentor voltage was decreased to 50 V to aid in detection of CoA ligated products.

Identification of AsuB2 flavin cofactor. Purified AsuB2 was boiled for ten minutes and precipitated protein was removed by centrifugation (10,000 x g, 2 min). The supernatant was analyzed by LC-UV-MS and compared to authentic standards of FAD and FMN. LC-UV-MS analysis was performed on an Agilent 6120 single quadrupole LC/MS equipped with an Agilent Eclipse Plus C18 column (4.6 x 100 mm). A linear gradient of 2-98% CH_3CN with 0.1% formic acid (v/v) over 20 minutes in H_2O with 0.1% formic acid (v/v) with a flow rate of 0.5 mL/min was used. Absorbance was monitored at 450 nm. An absorbance scan of the intact protein was collected using a Molecular Devices SpectraMax M2 plate reader. Scans were collected from 200-750 nm with a 5 nm step size.

Enzymatic dehydrogenation and dehydration of Acyl-CoAs by AsuB2. Coupled enzymatic reactions were performed at room temperature for two hours in 50 µL of 25 mM ammonium bicarbonate (pH 7.5) containing 1mM $MgCl_2$, 1 mM ATP, 1 mM CoA, 1 mM FAD, 2 mM acid substrate, 20 µM $AsuB1_C$, with and without 20 µM AsuB2. Reactions were quenched with an equal volume of 10% TFA, precipitated protein was removed by centrifugation (10,000 x g, 2 min) and the supernatant was used for analysis. LC-UV-HRMS analysis was performed on an Agilent technologies 6545 Accurate-Mass Q-TOF LC-MS instrument with an Agilent Eclipse Plus C18 column (4.6 x 100 mm). A linear gradient of 10-35% CH_3CN with 0.1% formic acid (v/v) over 30 minutes in H_2O with 0.1% formic acid (v/v) with a flow rate of 0.5 mL/min was used. Absorbance was measured at 260 nm. The fragmentor voltage was decreased to 50 V to aid in detection of CoA ligated products.

Determination of the FAD dependence of AsuB2 catalyzed dehydration. Apo-AsuB2 was purified from *S. asukabaensis* and appeared colorless. To generate holo-AsuB2 the protein was incubated with 5 mM FAD for 30 minutes at room temperature. A control was incubated with water under the same conditions. Each form of AsuB2 as then used in coupled assays. Coupled enzymatic reactions were performed at room temperature for two hours in 100 µL of 25 mM ammonium bicarbonate (pH 7.5) containing 1mM $MgCl_2$, 1 mM ATP, 1 mM CoA, 2 mM acid substrate, 20 µM $AsuB1_C$, with 20 µM apo- or holo-AsuB2. Reactions were quenched with an equal volume of 10% TFA, precipitated protein was removed by centrifugation (10,000 x g, 2 min) and the supernatant was used for analysis. LC-UV-HRMS analysis was performed on an Agilent technologies 6545 Accurate-Mass Q-TOF LC-MS instrument with an Agilent Eclipse Plus C18 column (4.6 x 100 mm). A linear gradient of 10-35% CH_3CN with 0.1% formic acid (v/v) over 30 minutes in H_2O with 0.1% formic acid (v/v) with a flow rate of 0.5 mL/min was used. Absorbance was measured at 260 nm. The fragmentor voltage was decreased to 50 V to aid in detection of CoA ligated products.

Time course analysis of competing AsuB2 catalyzed dehydrogenation/dehydration reactions. Coupled enzymatic reactions were performed at room temperature for two hours in 500 µL of 25 mM ammonium bicarbonate (pH 7.5) containing 1mM $MgCl_2$, 1 mM ATP, 1 mM CoA, 1 mM FAD, 2 mM acid substrate, 20 µM $AsuB1_C$, with and without 4 µM AsuB2. At each time point (2, 10, 15, 30, and 60 minutes) 50 µL was removed and quenched with an equal volume of 10% TFA. Precipitated protein was removed by centrifugation (10,000 x g, 2 min) and the supernatant was used for analysis. LC-UV-HRMS analysis was performed on an Agilent technologies 6545 Accurate-Mass Q-TOF LC-MS instrument with an Agilent Eclipse Plus C18 column (4.6 x 100 mm). A linear gradient of 10-35% CH_3CN with 0.1% formic acid (v/v) over 30 minutes in H_2O with 0.1% formic acid (v/v) with a flow rate of 0.5 mL/min was used. Absorbance was measured at 260 nm. The fragmentor voltage was decreased to 50 V to aid in detection of CoA ligated products.

Determination of the product of AsuB2 dehydration reaction. Coupled enzymatic reactions were performed in 50 µL of 25 mM ammonium bicarbonate (pH 7.5) containing 1mM $MgCl_2$, 1 mM ATP, 1 mM CoA, 2 mM malonyl-CoA, 1 mM FAD, 2 mM acid substrate, 20 µM $AsuB1_C$, 20 µM AsuB2, and 20 µM HsPKS1. Reactions proceeded for two hours at room temperature and were extracted with two volumes of ethyl acetate, dried under nitrogen, and resuspended in 50 µL of methanol for analysis. LC-HRMS analysis was carried out on an Agilent 6545 quadrupole time

of flight LC/MS equipped with an Agilent Eclipse Plus C18 column (4.6 x 100 mm). A linear gradient of 30-98% CH3CN with 0.1% formic acid (v/v) over 30 min in H2O with 0.1% formic acid (v/v) at a flow rate of 0.5 mL/min was used. LC-HRMS results were compared to enzymatically produced standards of triketide lactone products.

Determination of the product of AsuB2 dehydrogenation reaction with 9. Coupled enzymatic reactions were performed in 50 µL of 25 mM ammonium bicarbonate (pH 7.5) containing 1mM $MgCl_2$, 1 mM ATP, 1 mM CoA, 2 mM malonyl-CoA, 1 mM FAD, 2 mM acid substrate, 20 µM $AsuB1_C$, 20 µM AsuB2, and 20 µM HsPKS1. Reactions proceeded for two hours at room temperature and were extracted with two volumes of ethyl acetate, dried under nitrogen, and resuspended in 50 µL of methanol for analysis. LC-HRMS analysis was carried out on an Agilent 6545 quadrupole time of flight LC/MS equipped with an Agilent Eclipse Plus C18 column (4.6 x 100 mm). A linear gradient of 30-98% CH3CN with 0.1% formic acid (v/v) over 30 min in H2O with 0.1% formic acid (v/v) at a flow rate of 0.5 mL/min was used. LC-HRMS results were compared to enzymatically produced standards of triketide lactone products.

Production of cyclohexenyl triketide lactone standards. Cyclohexenyl triketide lactone (TKL) standards were prepared using a coupled enzymatic reaction with $AsuB1_C$, HsPKS1 and three separate substrates: 1-cyclohexenylcarboxylic acid, 2-cyclohexenylcarboxylic acid, and 3-cyclohexenylcarboxylic acid. Authentic standards for 1-cyclohexenylcarboxylic acid and 3-cyclohexenylcarboxylic acid were available and used for analysis. 2-cyclohexenylcarboxylic acid was generated by the chemical dehydration of 3-hydroxycyclohexylcarboxylic acid. Specifically, 3-hydroxycyclohexylcarboxylic acid was dissolved in toluene and Amberlyst-15 catalyst was added in a 1:1 molar ratio. The reaction was refluxed overnight, the catalyst was removed by filtration, the toluene was removed by rotary evaporation and the sample was redissolved in methanol. Enzymatic production of the cyclohexenyl-TKL products proceeded at room temperature for two hours in 50 µL of 25 mM ammonium bicarbonate (pH 7.5) containing 1mM $MgCl_2$, 1 mM ATP, 1 mM CoA, 2 mM malonyl-CoA, 20 µM $AsuB1_C$, 20 µM HsPKS1 and 2 mM of either the pure acid standard, or a 2 mM equivalent of the chemical dehydration reaction product. Reactions were extracted with two volumes of ethyl acetate which was dried under nitrogen. The extract was resuspended in 50 µL of methanol for analysis. LC-HRMS analysis was carried out on an Agilent 6545 quadrupole time of flight LC/MS equipped with an Agilent Eclipse Plus C18 column (4.6 x 100 mm). A linear gradient of 30-98% CH3CN with 0.1% formic acid (v/v) over 30 min in H2O with 0.1% formic acid (v/v) at a flow rate of 0.5 mL/min was used. The chemical dehydration reaction was verified to produce 1-cyclohexenylcarboxylic acid, 2-cyclohexenylcarboxylic acid, and 3-cyclohexenylcarboxylic acid determined by the presence of each analogous TKL after enzymatic assay and LC-HRMS analysis. The LC-HRMS results of the enzymatic assays with authentic 1-cyclohexenylcarboxylic acid and 3-cyclohexenylcarboxylic acid verified this result and suggested the remaining peak was the 2-cyclohexenecarboxyl-TKL.

Determination of the isomerization activity of AsuB2. Coupled enzymatic reactions were performed in 50 µL of 25 mM ammonium bicarbonate (pH 7.5) containing 1mM $MgCl_2$, 1 mM ATP, 1 mM CoA, 2 mM malonyl-CoA, 1 mM FAD, 2 mM 1-cyclohexenylcarboxylic acid, 20 µM $AsuB1_C$, and 20 µM HsPKS1 with and without 20 µM AsuB2. Reactions proceeded for two hours at room temperature and were extracted with two volumes of ethyl acetate, dried under nitrogen, and resuspended in 50 µL of methanol for analysis. LC-HRMS analysis was carried out on an

Agilent 6545 quadrupole time of flight LC/MS equipped with an Agilent Eclipse Plus C18 column (4.6 x 100 mm). A linear gradient of 30-98% CH3CN with 0.1% formic acid (v/v) over 30 min in H2O with 0.1% formic acid (v/v) at a flow rate of 0.5 mL/min was used. LC-HRMS results were compared to the enzymatically produced standards of triketide lactone products.

Biosynthesis of cyclohexanecarboxyl-CoA in *E. coli*. Three plasmids, pETDuet-asuB1-asuB4, pCOLADuet-asuB3, and pCDFDuet-hspks1-asuB2, were constructed using restriction digest cloning. All three were transformed into chemically competent *E. coli* BL21 Gold (DE3) to yield strain DS4. Strains lacking one of the biosynthetic genes were also created this way and are tabulated in **Table S2**. All strains contained three plasmids and the respective cloning site was left empty if that gene was not included in the strain. Transformants were selected on LB agar plates supplemented with kanamycin (50 μg/mL), carbenicillin (100 μg/mL) and spectinomycin (50 μg/mL). Single colonies were inoculated into 2 mL of LB + antibiotics and grown overnight at 37 °C. This seed culture was used to inoculate 25 mL of fresh LB + antibiotics at 1% inoculum. The cultures were grown at 37 °C to OD_{600} = 0.4-0.6 before induction with 40 μM IPTG and the addition of shikimic acid at a final concentration of 1mM. After induction, the temperature was decreased to 20 °C, and compound production was allowed to proceed for 48 hours.

LC-HRMS Analysis of cyclohexanecarboxyl-triketide lactone production in *E. coli*. The production of the CHC-TKL *in vivo* was carried out the same way for all *E. coli* cultures. The 25 mL cultures were pelleted by centrifugation (4000 x g, 10 min) and the supernatant was extracted with two volumes of ethyl acetate. The solvent was removed by rotary evaporation and the residue was redissolved in methanol for LC-HRMS analysis. An enzymatic reaction containing commercially acquired cyclohexanecarboxyl-CoA (CoAla Biosciences) and HsPKS1 was used to generate a standard of the cyclohexanecarboxyl-triketide lactone product. Reactions were carried out in 50 μL of HEPES (pH 8) buffer for two hours at room temp and contained 1 mM cyclohexanecarboxyl-CoA, 2 mM malonyl-CoA and 20 μM HsPKS1. Reactions were extracted with two volumes of ethyl acetate, the solvent was dried under nitrogen and the residue was redissolved in methanol. LC-HRMS analysis of the enzymatically produced standard and culture extracts was performed on an Agilent technologies 6520 Accurate-Mass Q-TOF LC-MS instrument with an Agilent Eclipse Plus C18 column (4.6 x 100 mm). A linear gradient of 2-98% CH_3CN with 0.1% formic acid (v/v) over 30 minutes in H_2O with 0.1% formic acid (v/v) with a flow rate of 0.5 mL/min was used.

In vitro reconstitution of the final steps of CHC-CoA biosynthesis. Coupled enzymatic reactions were performed at room temperature for two hours in 100 μL of 25 mM ammonium bicarbonate (pH 7.5) containing 1mM $MgCl_2$, 1 mM ATP, 1 mM CoA, 1 mM FAD, 2 mM 3-hydroxycyclohexanecarboxylic acid, 20 μM $AsuB1_C$, 20 μM AsuB2, with and without 20 μM AsuB3. Reactions were quenched with an equal volume of 10% TFA. Precipitated protein was removed by centrifugation (10,000 x g, 2 min) and the supernatant was used for analysis. LC-UV-HRMS analysis was performed on an Agilent technologies 6545 Accurate-Mass Q-TOF LC-MS instrument with an Agilent Eclipse Plus C18 column (4.6 x 100 mm). A linear gradient of 10-35% CH_3CN with 0.1% formic acid (v/v) over 30 minutes in H_2O with 0.1% formic acid (v/v) with a flow rate of 0.5 mL/min was used. Absorbance was measured at 260 nm. The fragmentor voltage was decreased to 50 V to aid in detection of CoA ligated products.

Table S1. Oligonucleotides used in this study

Primer Name	Sequence (5' -> 3')	Description
F_B3_EcoRI	aagaattcgatgagccccgtcgccgaaca	Creation of Heterologous Expression Vectors
R_B3_HindIII	ataagctttcagccctcccggaccggcc	
F_chcB_NdeI	aaacatatggccgacaccgtgctcta	
R_chcB_XhoI	aactcgagtcagcgccccaggtacgtcg	
24461 B1 PSTI	aaactgcagatgcgcttaattgtcaaaca	
24461 B1 HindIII	tttaagctttcacgacccgtcctcgcctg	
24461 B4 NdeI	aaacatatgagccatgtcttccagcc	
24461 B4 XhoI	aactcgagtcacaacgcctcctggaggt	
F_B2_NdeI	aaacatatggccgacaccgtgctcta	
R_B2_XhoI	aactcgagtcacaggccggcctccgcac	
F_AsuB1_dws	ggtattgagggtcgc atgcatctcacgctcaggcc	Expression of AsuB1
R_AsuB1_dws	agaggagagttagagcctcatgcgtgctgctcctcgg	
3298_B2_F	ggtattgagggtcgc atgacagtcgacatcatcga	Expression of AsuB2 homolog from NRRL-B-3298
3298_B2_R	agaggagagttagagcc tcatcgcgcgccctcccacc	
F_AsuB3_dws	ggtattgagggtcgc atgagccccgtcgccgaacag	Expression of AsuB3
R_AsuB3_dws	agaggagagttagagcctcagccctcccggaccggcc	
F_AsuB4_dws	ggtattgagggtcgc atgctgaagcacgttttccgc	Expression of AsuB4
R_AsuB4_dws	agaggagagttagagcctcagcggcccggcgtcggaa	
ChcB_dws_F	ggtattgagggtcgc atggccgacaccgtgctcta	Expression of ChcB
ChcB_dws_R	agaggagagttagagcc tcagcgccccaggtacgtcg	
B1_CoA_pet30_F	ggtattgagggtcgc atgtccgtcgaatcggccgc	Expression of AsuB1C
B1_CoA_pet30_R	agaggagagttagagcctcatgcgtgctgctcctcgg	
B1_N_pet30_F	gctccggtattgagggtcgc atgcatctcacgctcaggcc	Expression of AsuB1N with separate truncation sites
B1_N-2_pet30_R	gccagaggagagttagagcc tcaccggagcccgaggcc	
B1_N-3_pet30_R	gccagaggagagttagagcc tcacgcggccgattcgacgg	
B1_N-1_pet30_R	gccagaggagagttagagcc tcacaggaaggccgggtagg	
1627_B1_F	ggtattgagggtcgc atgcatcttcttgtcaagggaa	Expression of AsuB1 homolog from NRRL-B-1627
1627_B1_R	aggagagttagagcc ttacttgcttccctcctcgcgc	
3298_B1_F	ggtattgagggtcgc atgcaccttctgctcgaacgca	Expression of AsuB1 homolog from NRRL-B-3298
3298_B1_R	aggagagttagagcc ttatgcgctctgcgcctccgga	
24461_B1_F	ggtattgagggtcgc atgcgcttaattgtcaaacagg	Expression of AsuB1 homolog from NRRL-B-24461
24461_B1_R	aggagagttagagcc ttacgacccgtcctcgcctgtg	

Table S2. Plasmids used in this study

Plasmid	Description	Reference
pART1361	Cosmid containing the asukamycin biosynthetic gene cluster, used as PCR template	[1]
pET30a	Expression plasmid	Novagen
pETDuet-1	Expression plasmid	Novagen
pCDFDuet-1	Expression Plasmid	Novagen
pCOLADuet-1	Expression plasmid	Novagen
pET30-asuB1-24461	pET30 derivative for purification of *A. albata* AsuB1 from *E. coli*	This Study
pET30-asuB2-3298	pET30 derivative for purification of AsuB2 homolog from NRRL-B-3298 from *E. coli*	This Study
pET30-asuB3	pET30 derivative for purification of AsuB3 from *E. coli*	This Study
pCDF-hspks1	pET30 derivative for purification of HsPKS1 from *E. coli*	This Study
pETDuet-asuB1-asuB4	pETDuet derviative for heterologous expression of AsuB1 and AsuB4 from A. albata NRRL B-24461	This Study
pCDFDuet-hspks1-asuB2	pCDFDuet derivative for heterologous expression of HsPKS1 and AsuB2	This Study
pCOLADuet-asuB3	pCOLADuet derivative for heterologous expression of AsuB3	This Study
pET30-asuB1C	pET30 derivative for purification of AsuB1C from *E. coli*	This Study
pET30-asuB1N-3298	pET30 derivative for purification of AsuB1N homolog from NRRL-B-3298 from *E. coli*	This Study
pET30-asuB1N-24461	pET30 derivative for purification of AsuB1N homolog from NRRL-B-24461 from *E. coli*	This Study
pET30-asuB1N-1627	pET30 derivative for purification of AsuB1N homolog from NRRL-B-1627 from *E. coli*	This Study

Table S3. Strains used in this study

Strain	Description	Reference
A. albata NRRL-B-24461	gDNA isolation for AsuB1234 homologous gene cluster	[2]
L. aerocolonigenes NRRL-B-3298	gDNA isolation for AsuB1234 homologous gene cluster	[3]
S. sulphureus NRRL-B-1627	gDNA isolation for AsuB1234 homologous gene cluster	[4]
E. coli BL21 Gold (DE3)	Heterologous Expression and Overproduction of Recombinant Protein	Agilent Technologies
E. coli XL1 Blue	General Cloning Host	Agilent Technologies
DS4 - E. coli BL21 Gold DE3)	Heterologous Expression of CHC-TKL, contains *asuB1234*	This Study
DS7 - E. coli BL21 Gold (DE3)	Heterologous Expression of CHC-TKL, lacks *asuB3*	This Study
DS8 - E. coli BL21 Gold (DE3)	Heterologous Expression of CHC-TKL, lacks *asuB1*	This Study
DS9 - E. coli BL21 Gold (DE3)	Heterologous Expression of CHC-TKL, lacks *asuB4*	This Study
DS10 - E. coli BL21 Gold (DE3)	Heterologous Expression of CHC-TKL, lacks *asuB2*	This Study

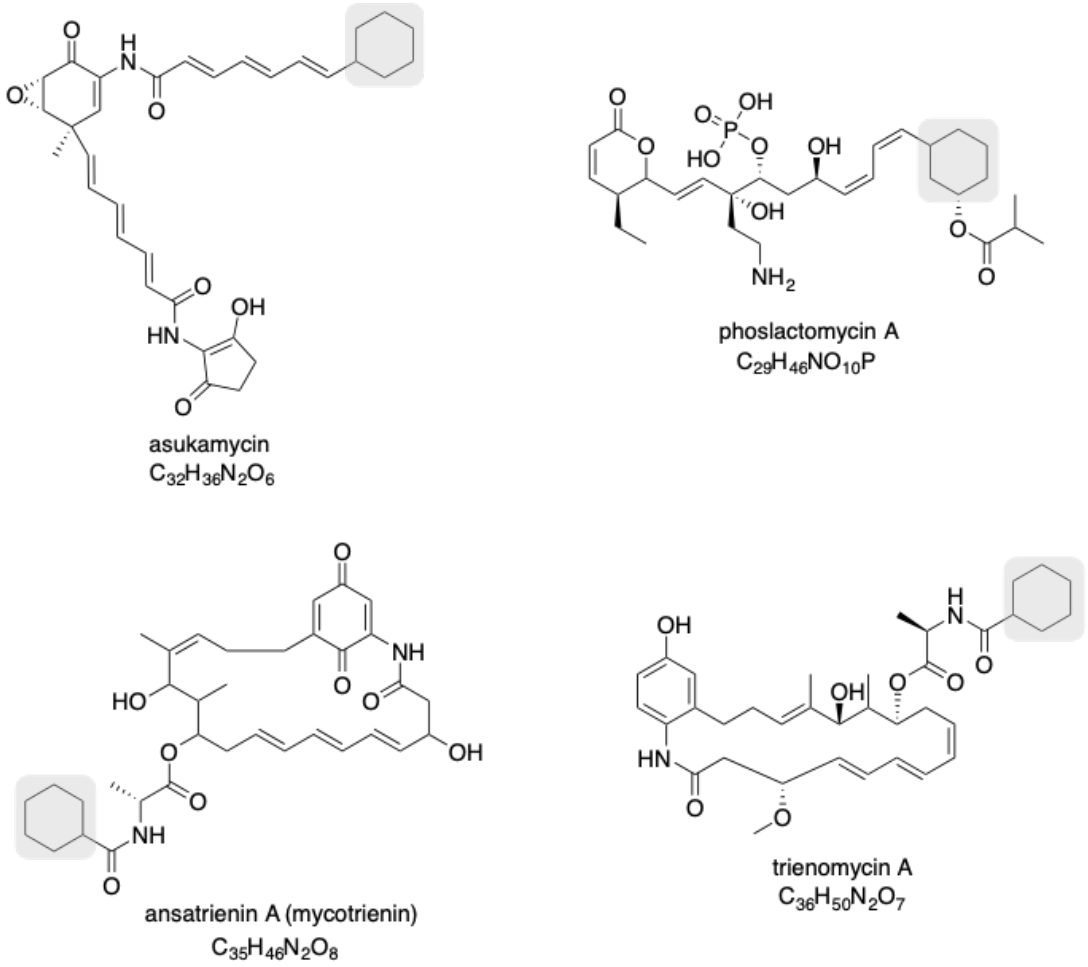

Figure S1. Major natural product scaffolds that contain the cyclohexane carboxylic acid moiety.[1,5–7]

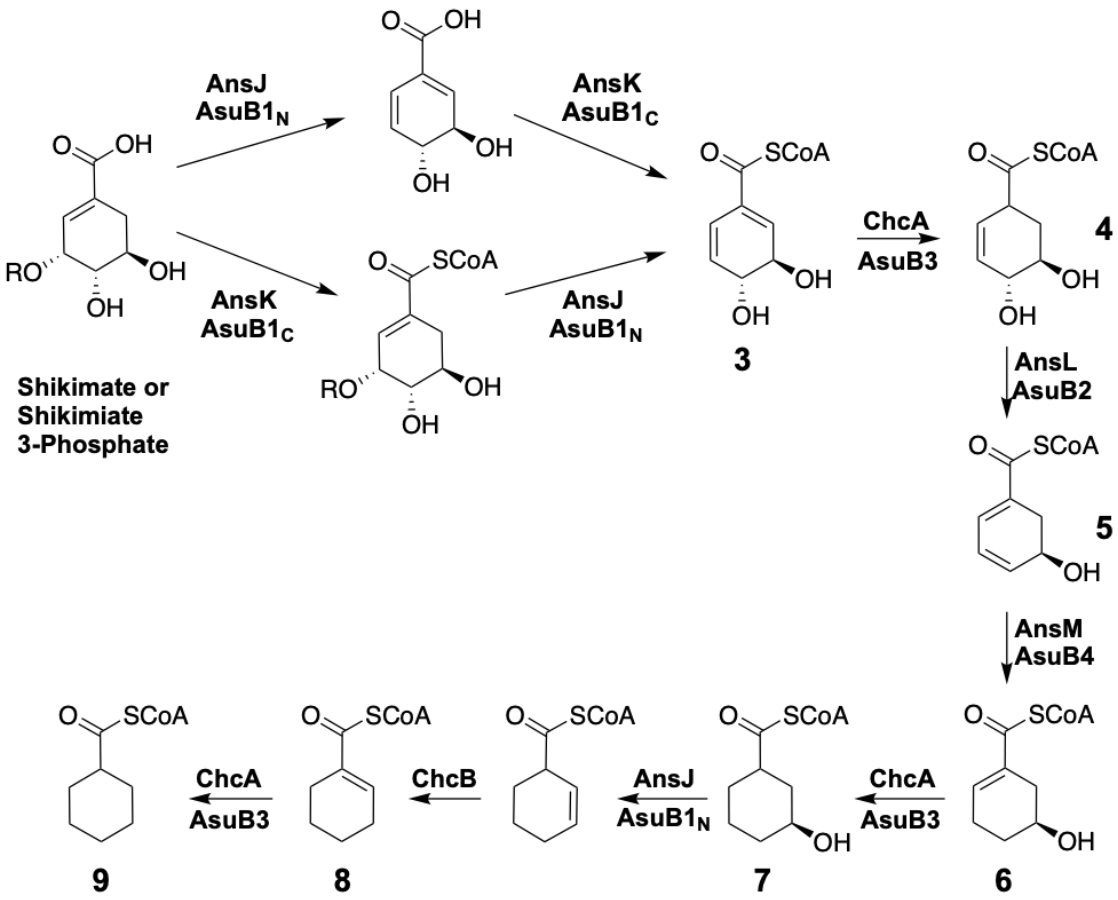

Figure S2. Previously proposed mechanism for the formation of **9** from shikimate or shikimate-3-phosphate.[8]

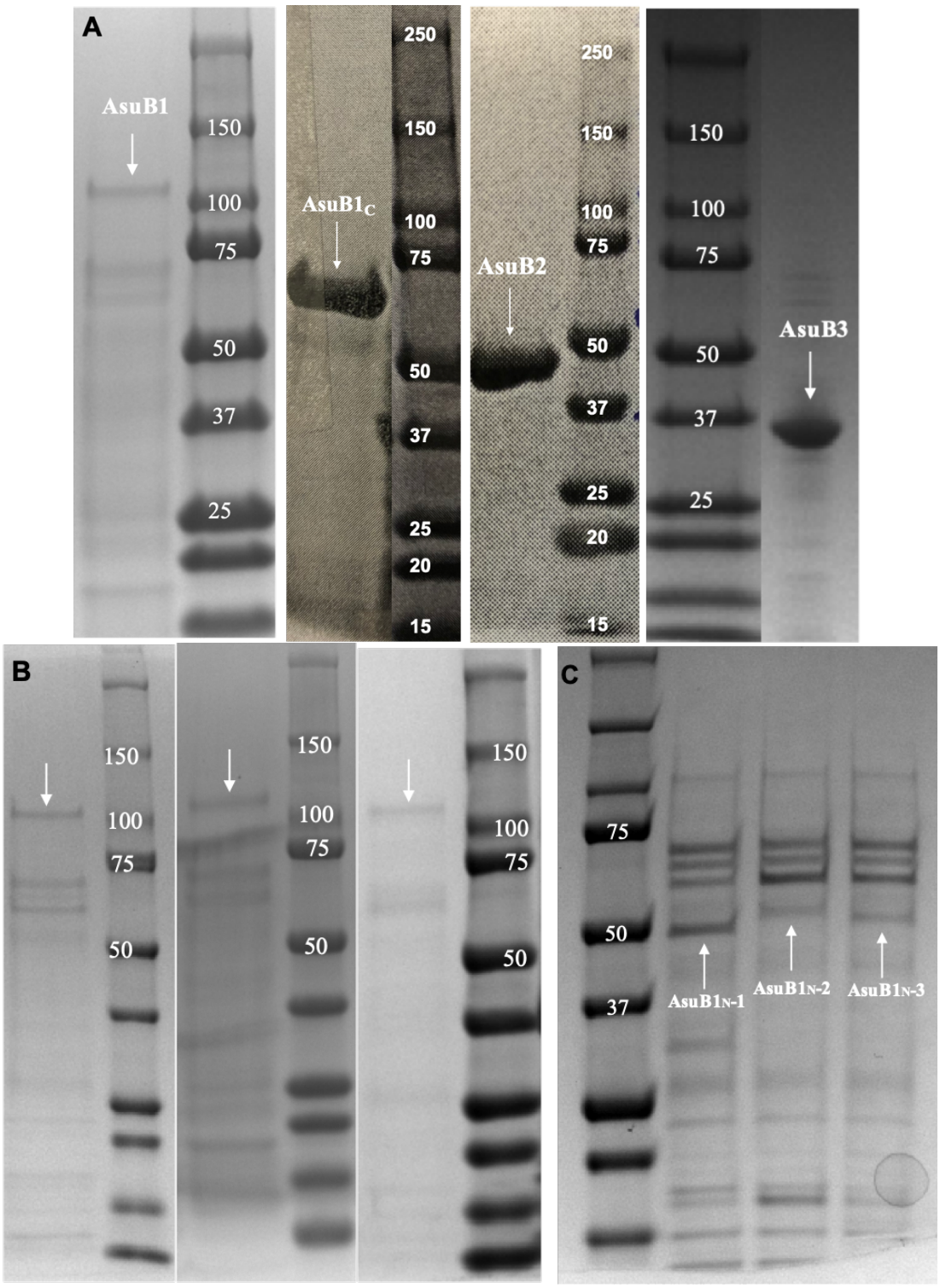

Figure S3. SDS-PAGE analysis of cyclohexanecarboxylic acid biosynthetic enzymes purified in this study. (A) Recombinant proteins used for *in vitro* biochemical assays. (B) Solubility screen of AsuB1 homologs for attempted *in vitro* characterization. From left to right: *S. sulphureus* NRRL-B-1627, *L. aerocolonigenes* NRRL-B-3298, *A. albata* NRRL-B-24461. (C) Solubility screen of different truncation points for recombinant expression of AsuB1$_N$.

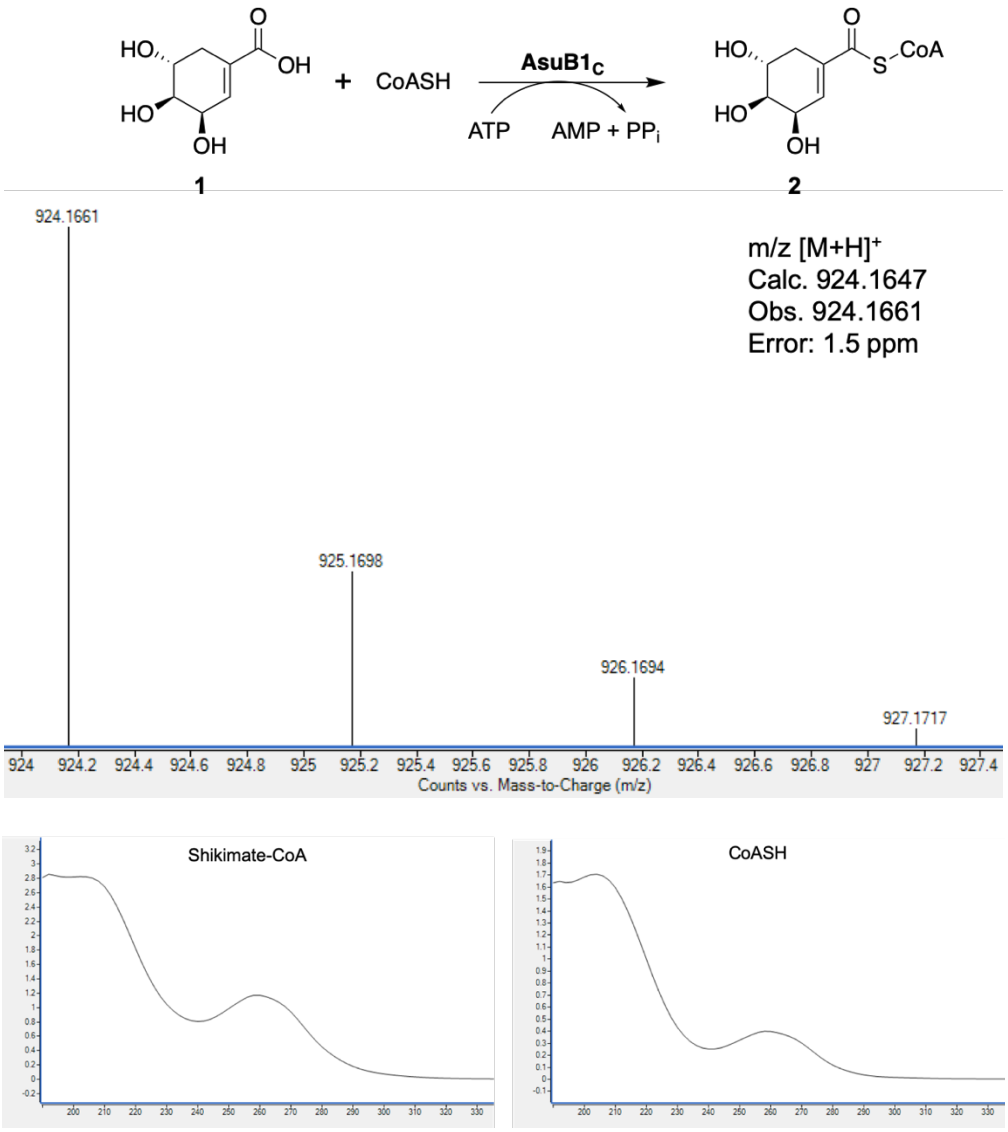

Figure S4. LC-UV-HRMS analysis of product of shikimate CoA ligation by AsuB1$_C$.

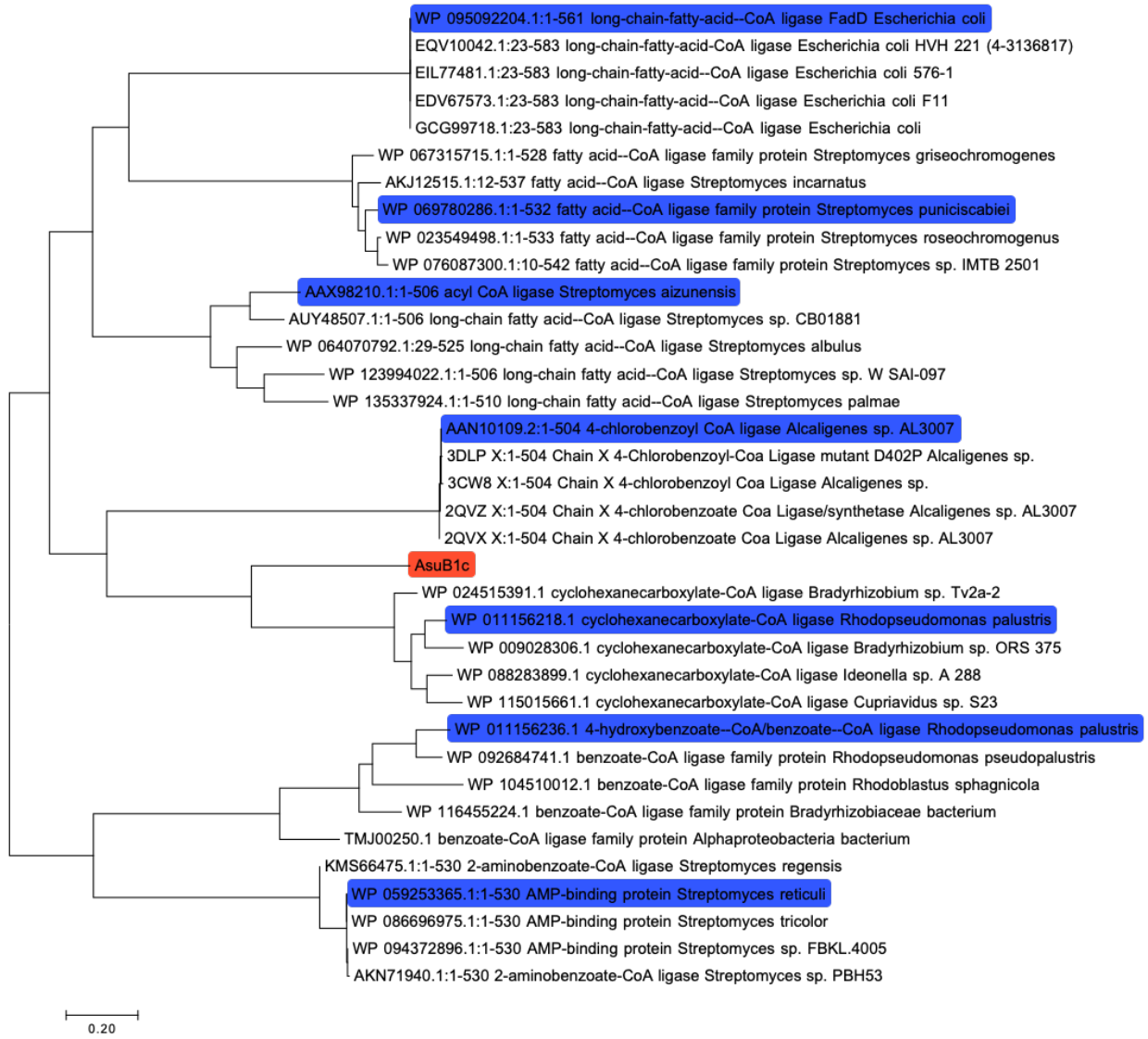

Figure S5. Phylogenetic analysis of AsuB1$_C$ (red) compared to selected CoA ligases highlighted in blue.[9–14] The evolutionary history was inferred by using the Maximum Likelihood method based on the JTT matrix-based model.[15] The tree with the highest log likelihood (-13659.10) is shown. Initial tree(s) for the heuristic search were obtained automatically by applying Neighbor-Join and BioNJ algorithms to a matrix of pairwise distances estimated using a JTT model, and then selecting the topology with superior log likelihood value. The tree is drawn to scale, with branch lengths measured in the number of substitutions per site. The analysis involved 36 amino acid sequences. All positions containing gaps and missing data were eliminated. There were a total of 435 positions in the final dataset. Evolutionary analyses were conducted in MEGA7.[16]

	Substrate	K_m (μM)	k_{cat} (min^{-1})
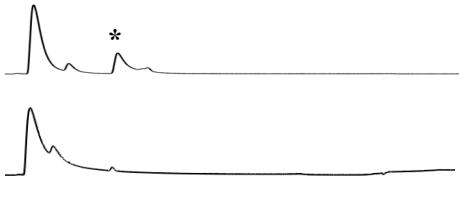	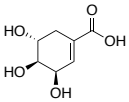	360.7 ± 35.48	1.75 ± 0.035
	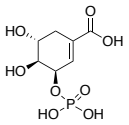	No Rxn	
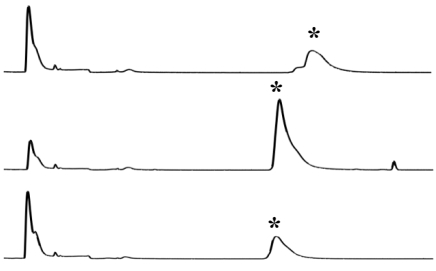		16.17 ± 1.65	1.67 ± 0.046
		16.67 ± 2.45	1.66 ± 0.067
		12.06 ± 1.15	1.63 ± 0.037
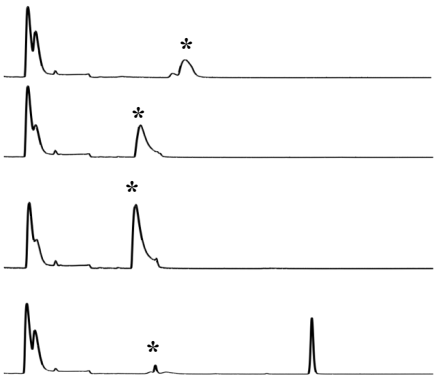		46.00 ± 7.34	1.39 ± 0.038
	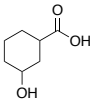	78.37 ± 13.29	1.54 ± 0.049
	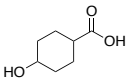	25.5 ± 2.40	1.48 ± 0.022
	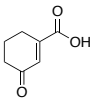	43.02 ± 2.79	5.64 ± 0.11
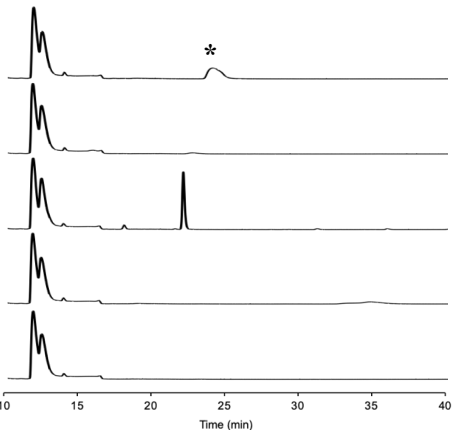	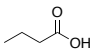	319.7 ± 44.51	1.55 ± 0.051
		No Rxn	
	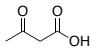	No Rxn	
	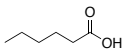	No Rxn	
	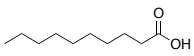	No Rxn	

	Substrate	K_m (μM)	k_{cat} (min^{-1})
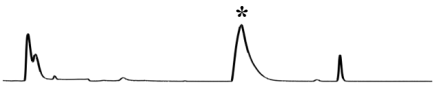		30.91 ± 4.56	1.53 ± 0.037
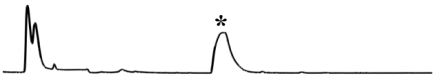		564.60 ± 99.3	5.22 ± 0.22
	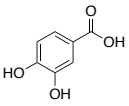	464.4 ± 43.59	2.50 ± 0.062
	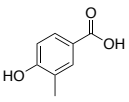	524.2 ± 36.22	1.01 ± 0.019
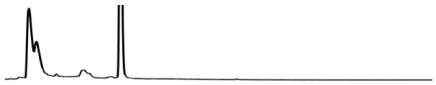	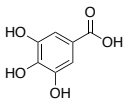	No Rxn	
	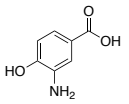	No Rxn	
	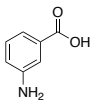	No Rxn	
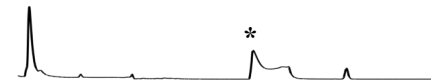	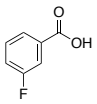	48.59 ± 3.54	3.05 ± 0.059
	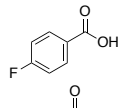	226.0 ± 28.08	3.06 ± 0.13
	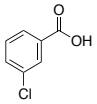	166.7 ± 12.55	2.89 ± 0.055
	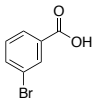	836.3 ± 63.61	5.55 ± 0.17
	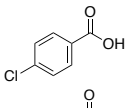	No Rxn	
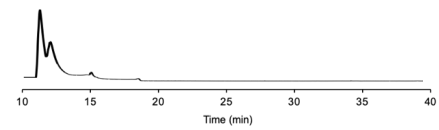	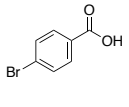	No Rxn	

Figure S6. LC-UV-MS and kinetics parameters of AsuB1$_C$ substrate scope. HPLC traces (260 nm) are shown for AsuB1$_C$ reactions with each acid substrate. An asterix indicates a peak that was verified by LC-MS to be the expected product. No rxn indicates that there was no new peak observed in the UV analysis. Kinetic analysis was carried out with a coupled spectrophotometric assay as described.

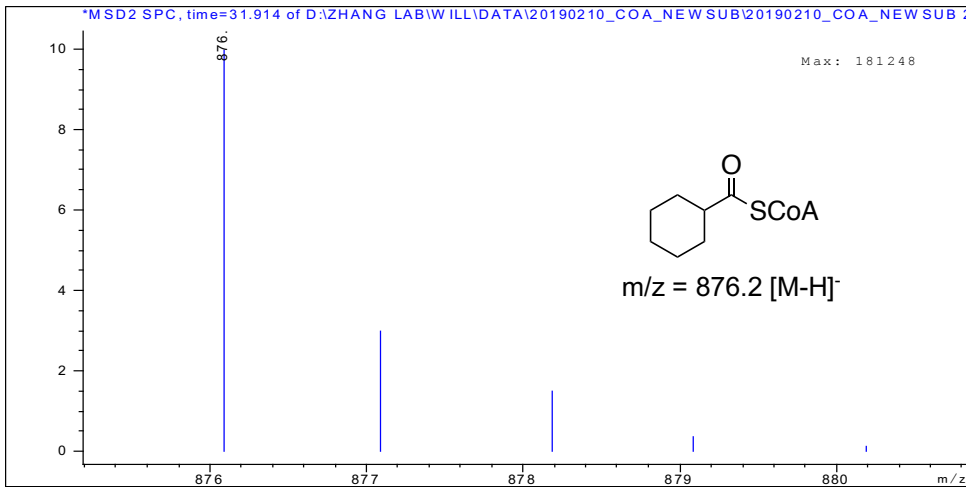
*MSD2 SPC, time=31.914 of D:\ZHANG LAB\WILL\DATA\20190210_COA_NEWSUB\20190210_COA_NEWSUB
Max: 181248
876.
O
SCoA
m/z = 876.2 [M-H]-
m/z

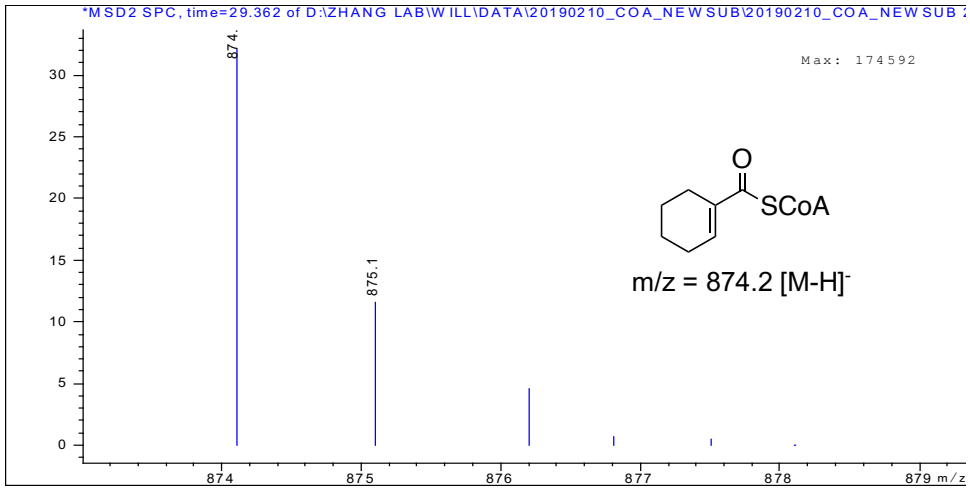
*MSD2 SPC, time=29.362 of D:\ZHANG LAB\WILL\DATA\20190210_COA_NEWSUB\20190210_COA_NEWSUB
Max: 174592
874.
875.1
O
SCoA
m/z = 874.2 [M-H]-
m/z

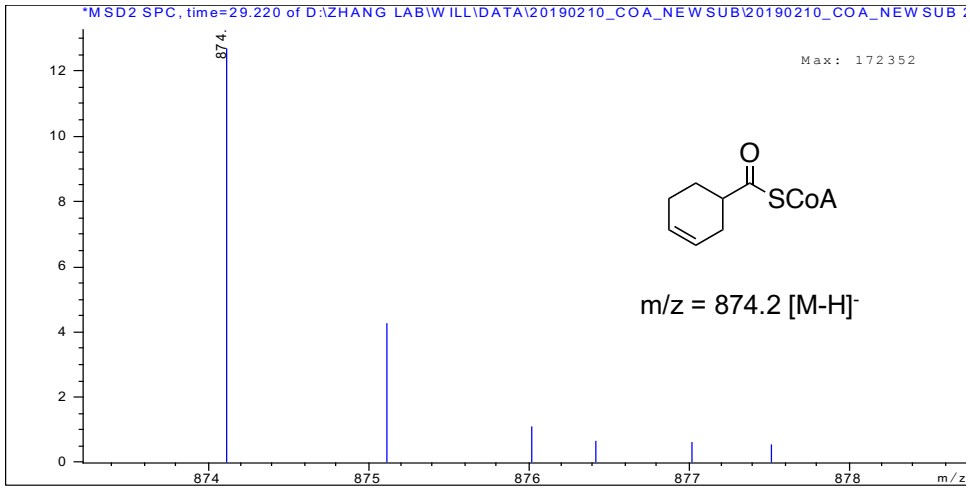
*MSD2 SPC, time=29.220 of D:\ZHANG LAB\WILL\DATA\20190210_COA_NEWSUB\20190210_COA_NEWSUB
Max: 172352
874.
O
SCoA
m/z = 874.2 [M-H]-
m/z

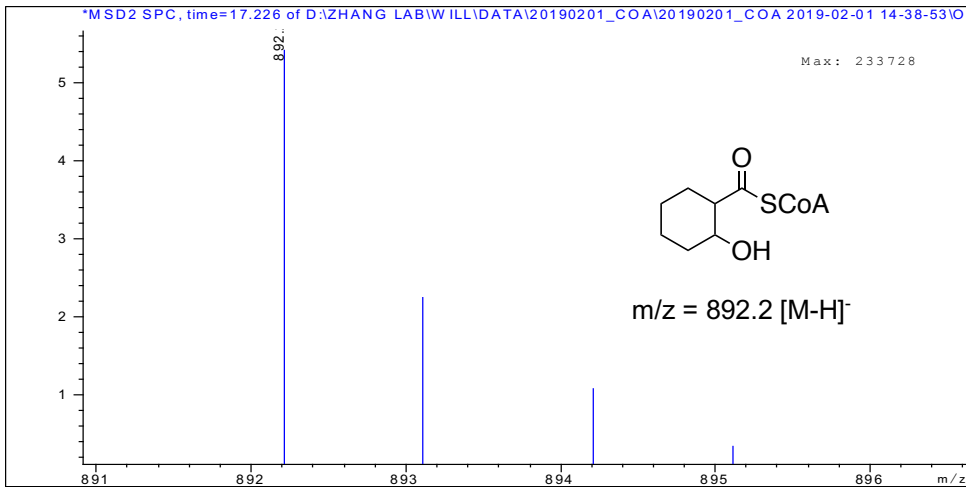
*MSD2 SPC, time=17.226 of D:\ZHANG LAB\WILL\DATA\20190201_COA\20190201_COA 2019-02-01 14-38-53\O
Max: 233728
892.
O
SCoA
OH
m/z = 892.2 [M-H]-
m/z

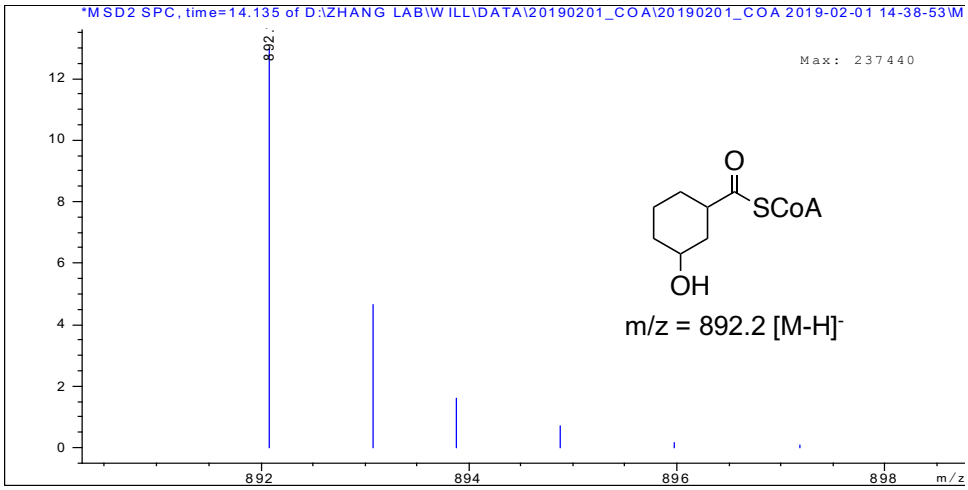
*MSD2 SPC, time=14.135 of D:\ZHANG LAB\WILL\DATA\20190201_COA\20190201_COA 2019-02-01 14-38-53\M
Max: 237440
892.
O
SCoA
OH
m/z = 892.2 [M-H]-
m/z

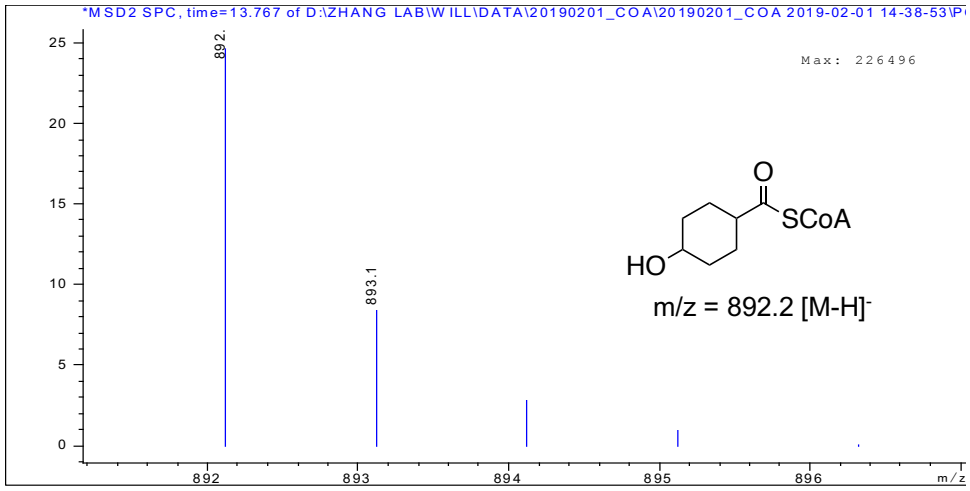
*MSD2 SPC, time=13.767 of D:\ZHANG LAB\WILL\DATA\20190201_COA\20190201_COA 2019-02-01 14-38-53\P
Max: 226496
892.
893.1
O
SCoA
HO
m/z = 892.2 [M-H]-
m/z

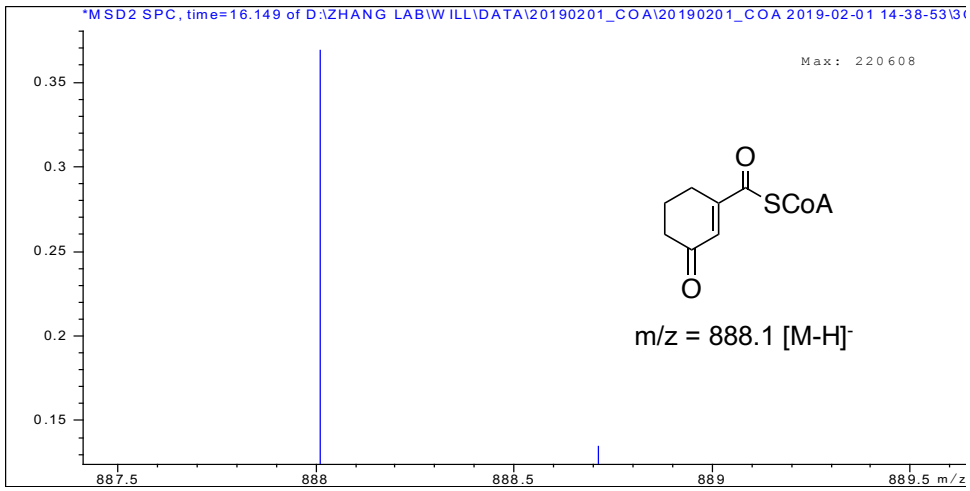
*MSD2 SPC, time=16.149 of D:\ZHANG LAB\WILL\DATA\20190201_COA\20190201_COA 2019-02-01 14-38-53\3
Max: 220608
0.35
0.3
0.25
0.2
0.15
887.5
888
888.5
889
889.5 m/z
O
SCoA
O
m/z = 888.1 [M-H]-

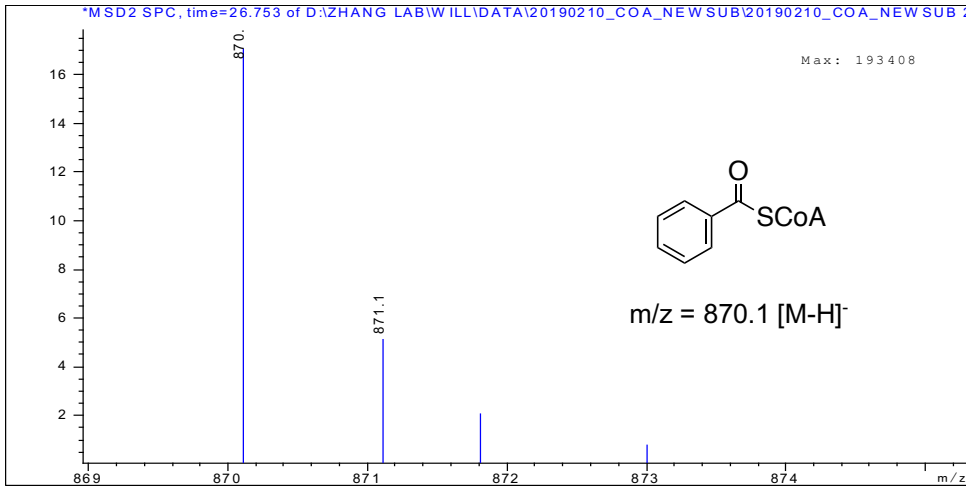
*MSD2 SPC, time=26.753 of D:\ZHANG LAB\WILL\DATA\20190210_COA_NEWSUB\20190210_COA_NEWSUB
Max: 193408
870.
871.1
16
14
12
10
8
6
4
2
869
870
871
872
873
874
m/z
O
SCoA
m/z = 870.1 [M-H]-

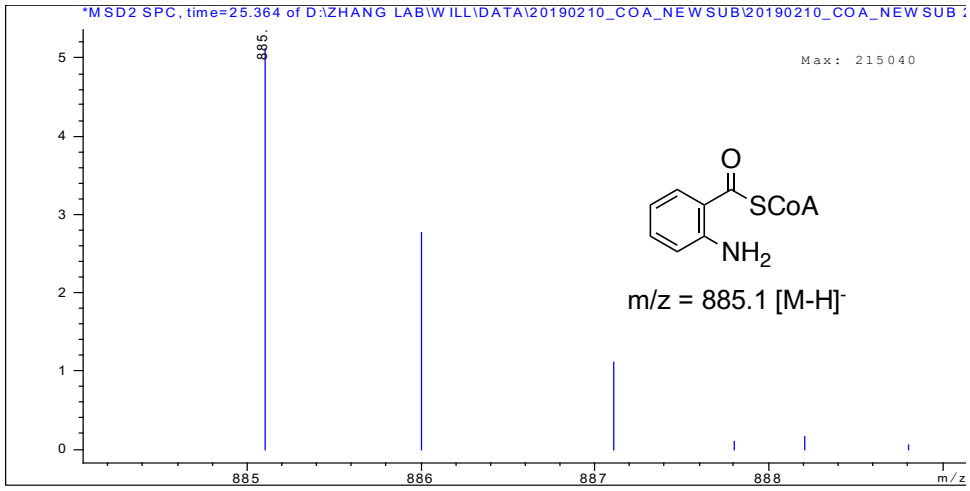
*MSD2 SPC, time=25.364 of D:\ZHANG LAB\WILL\DATA\20190210_COA_NEWSUB\20190210_COA_NEWSUB
Max: 215040
885.
5
4
3
2
1
0
885
886
887
888
m/z
O
SCoA
NH2
m/z = 885.1 [M-H]-

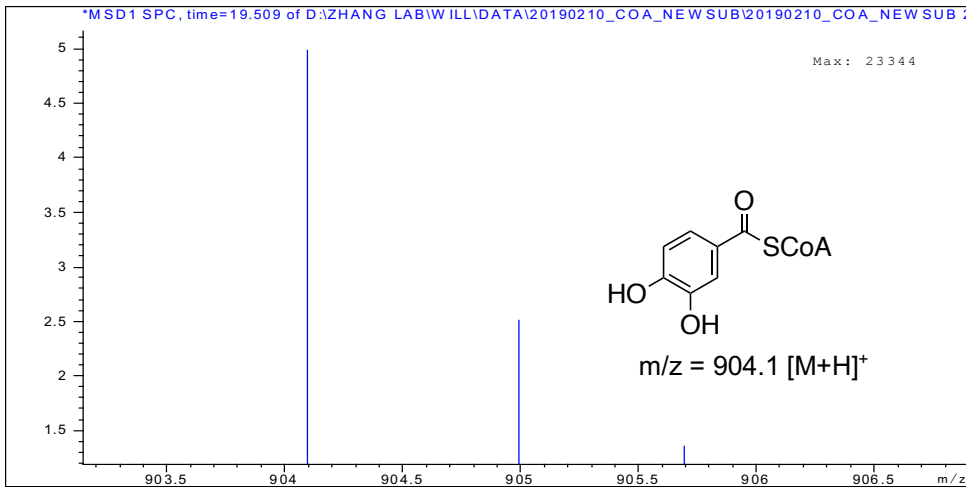
*MSD1 SPC, time=19.509 of D:\ZHANG LAB\WILL\DATA\20190210_COA_NEWSUB\20190210_COA_NEWSUB
Max: 23344
5
4.5
4
3.5
3
2.5
2
1.5
903.5
904
904.5
905
905.5
906
906.5
m/z
O
SCoA
HO
OH
m/z = 904.1 [M+H]+

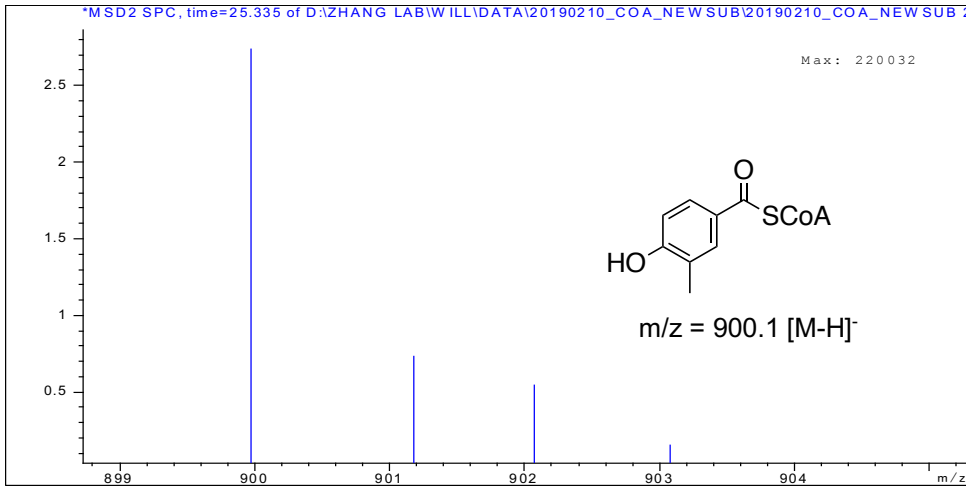
*MSD2 SPC, time=25.335 of D:\ZHANG LAB\WILL\DATA\20190210_COA_NEWSUB\20190210_COA_NEWSUB
Max: 220032
2.5
2
1.5
1
0.5
899
900
901
902
903
904
m/z
O
SCoA
HO
m/z = 900.1 [M-H]-

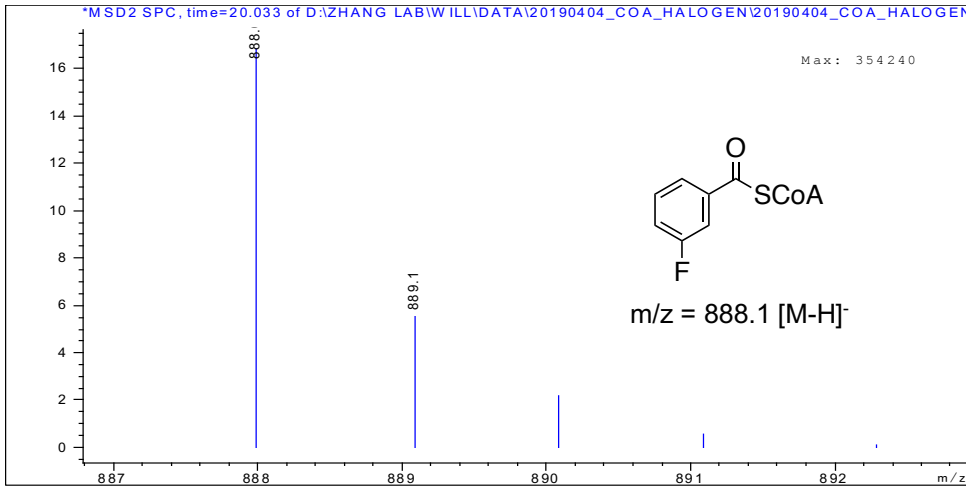
*MSD2 SPC, time=20.033 of D:\ZHANG LAB\WILL\DATA\20190404_COA_HALOGEN\20190404_COA_HALOGEN
Max: 354240
888.
889.1
16
14
12
10
8
6
4
2
0
887
888
889
890
891
892
m/z
O
SCoA
F
m/z = 888.1 [M-H]-

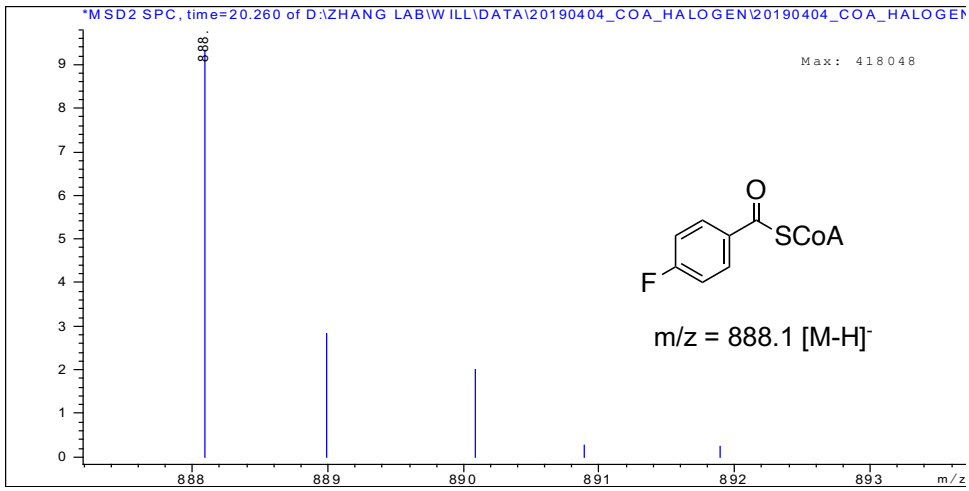
*MSD2 SPC, time=20.260 of D:\ZHANG LAB\WILL\DATA\20190404_COA_HALOGEN\20190404_COA_HALOGEN
Max: 418048
888.
O
SCoA
F
m/z = 888.1 [M-H]-
m/z

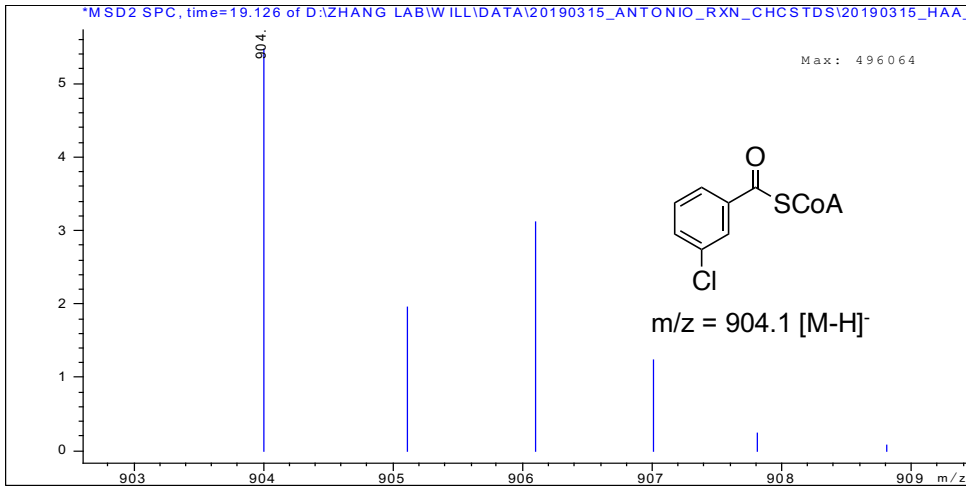
*MSD2 SPC, time=19.126 of D:\ZHANG LAB\WILL\DATA\20190315_ANTONIO_RXN_CHCSTDS\20190315_HAA
Max: 496064
904.
O
SCoA
Cl
m/z = 904.1 [M-H]-
m/z

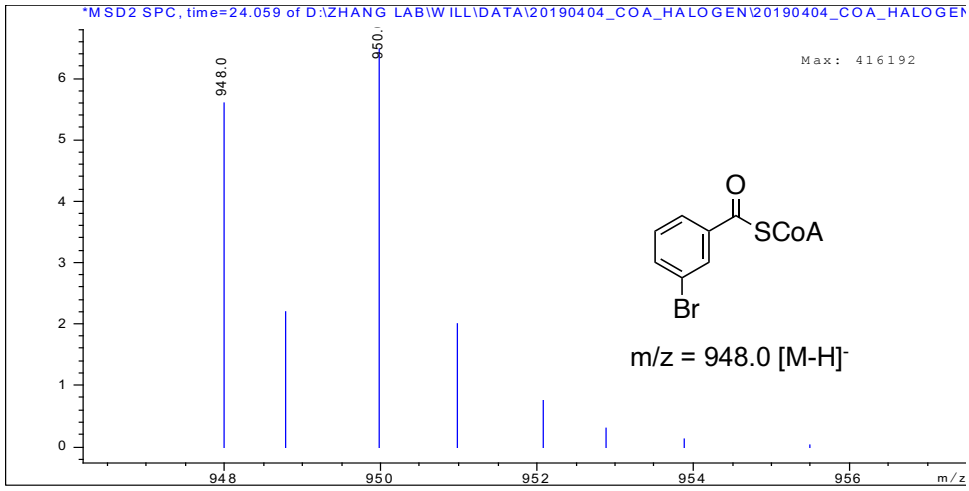
*MSD2 SPC, time=24.059 of D:\ZHANG LAB\WILL\DATA\20190404_COA_HALOGEN\20190404_COA_HALOGEN
Max: 416192
948.0
950.
O
SCoA
Br
m/z = 948.0 [M-H]-
m/z

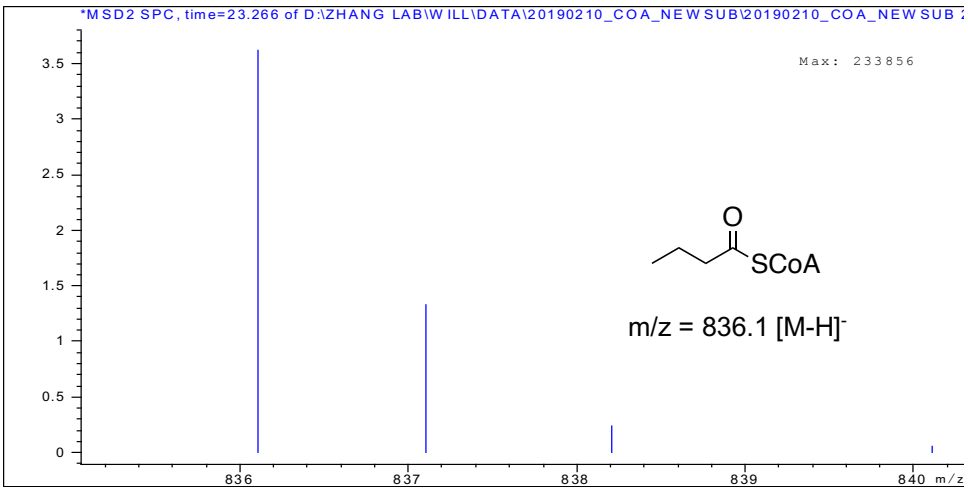

Figure S7. LC-MS analysis of acyl-CoA products produced by AsuB1$_C$ *in vitro* reactions.

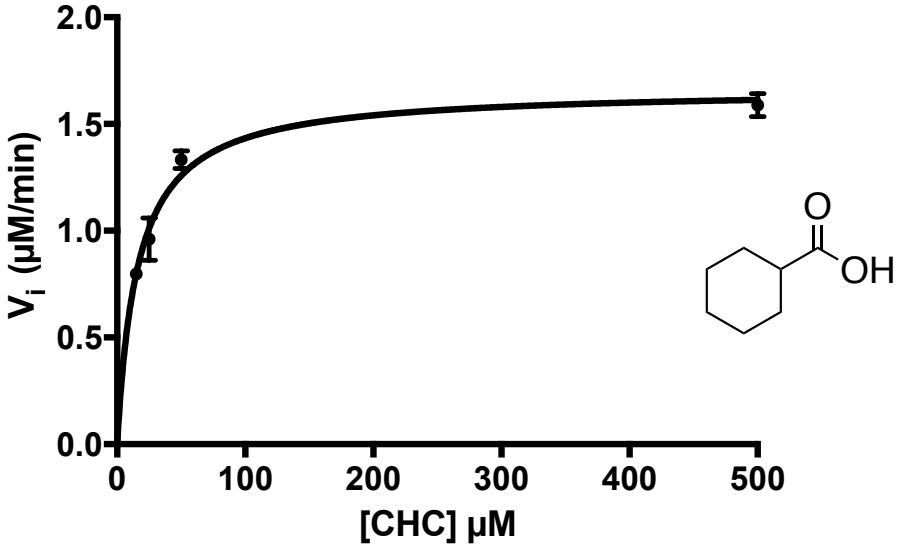
2.0
1.5
1.0
0.5
0.0
V_i (µM/min)
0
100
200
300
400
500
[CHC] µM
O
OH

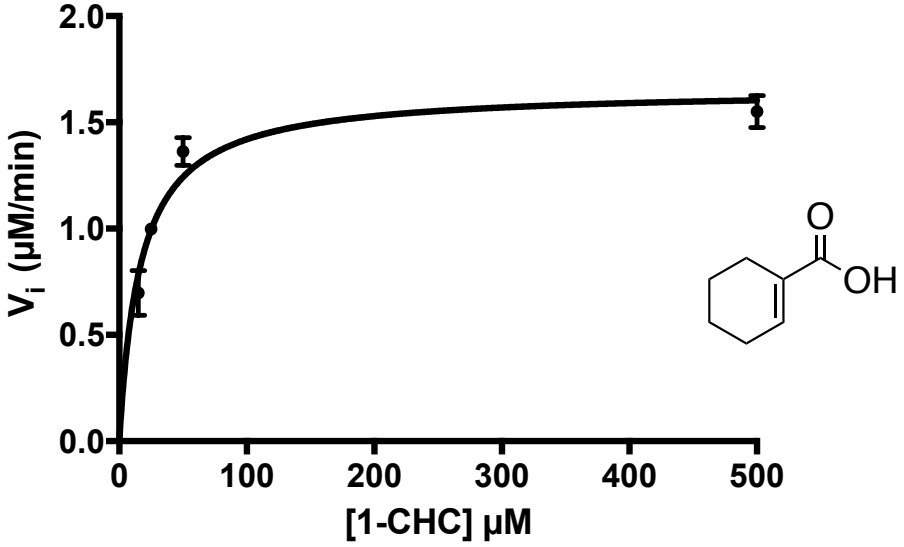
2.0
1.5
1.0
0.5
0.0
V_i (µM/min)
0
100
200
300
400
500
[1-CHC] µM
O
OH

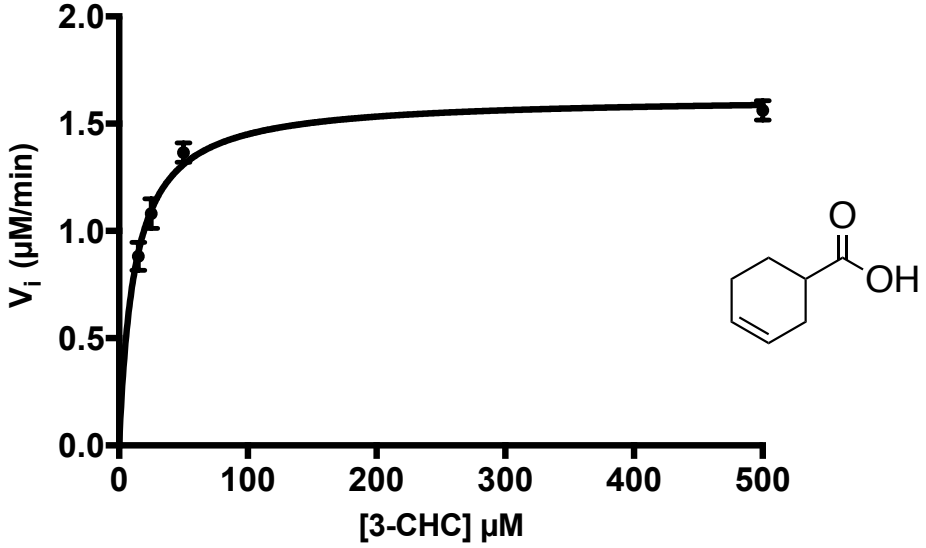
2.0
1.5
1.0
0.5
0.0
V_i (µM/min)
0
100
200
300
400
500
[3-CHC] µM
O
OH

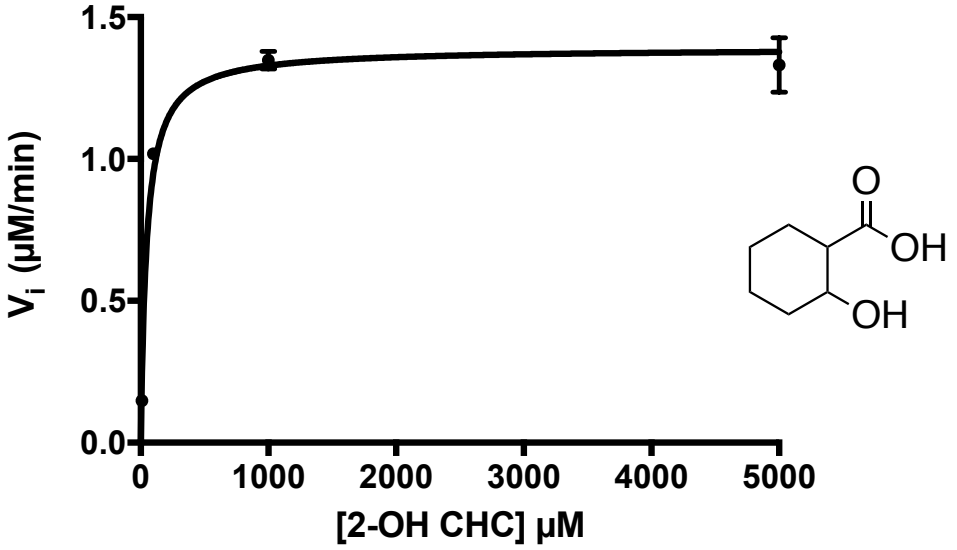
1.5
1.0
0.5
0.0
V_i (µM/min)
0
1000
2000
3000
4000
5000
[2-OH CHC] µM
O
OH
OH

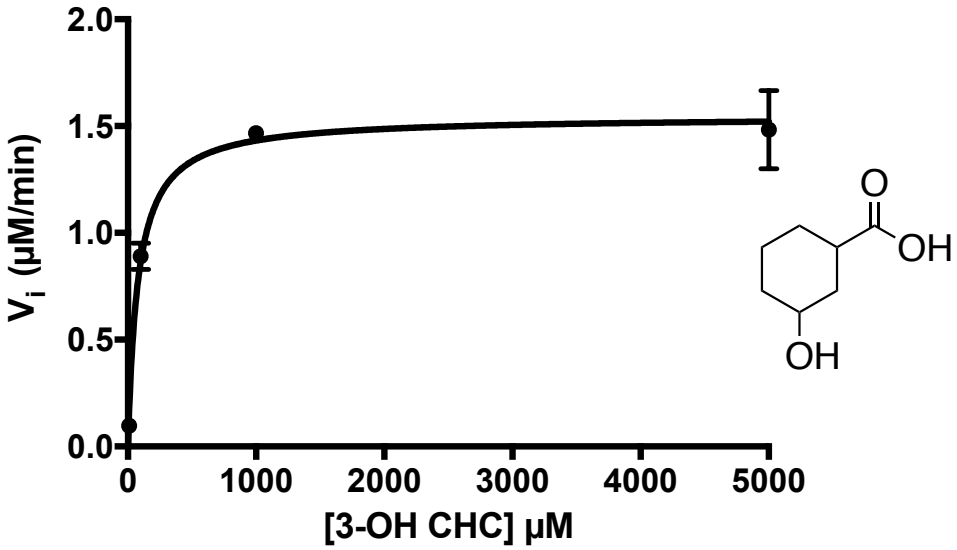
2.0
1.5
1.0
0.5
0.0
V_i (µM/min)
0
1000
2000
3000
4000
5000
[3-OH CHC] µM
O
OH
OH

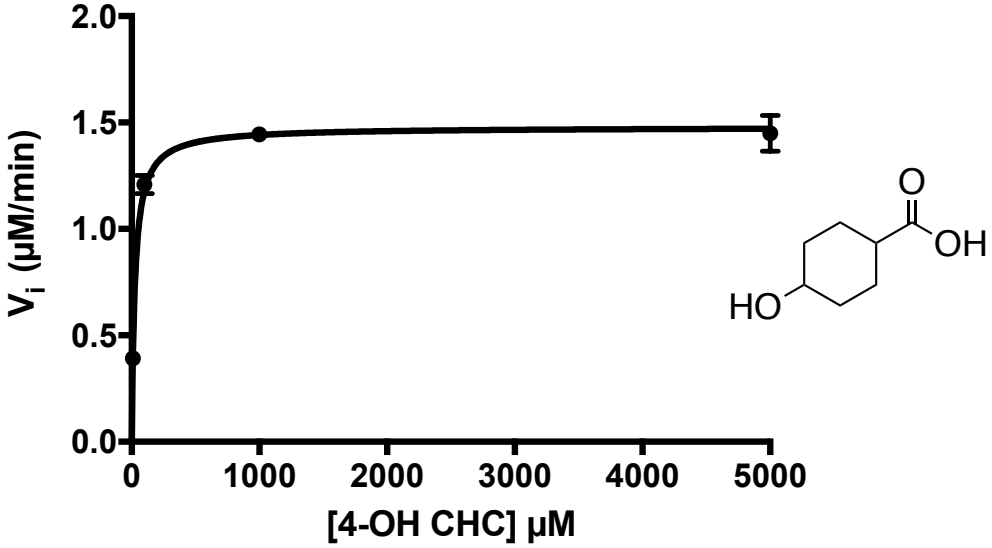
2.0
1.5
1.0
0.5
0.0
V_i (µM/min)
0
1000
2000
3000
4000
5000
[4-OH CHC] µM
O
OH
HO

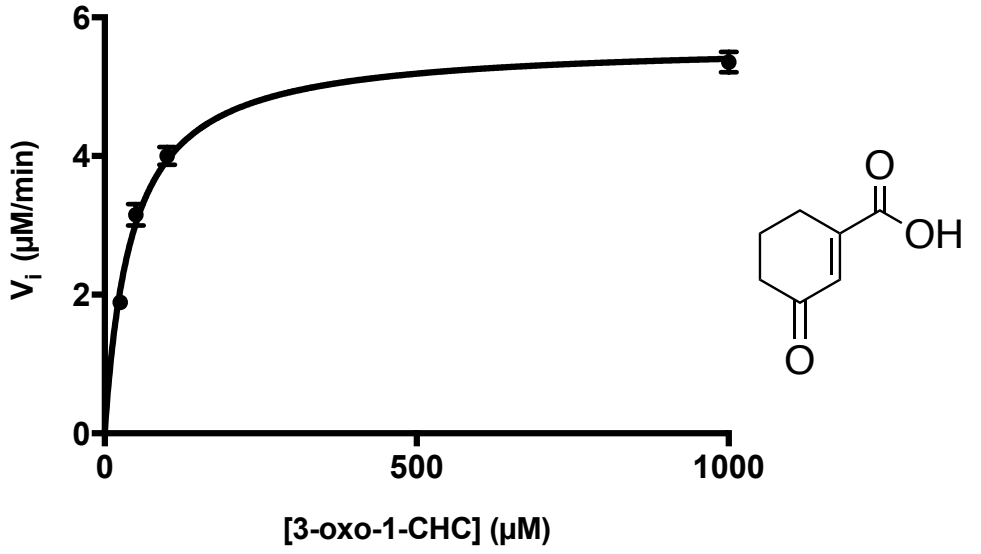
6
4
2
0
V_i (µM/min)
0
500
1000
[3-oxo-1-CHC] (µM)
O
OH
O

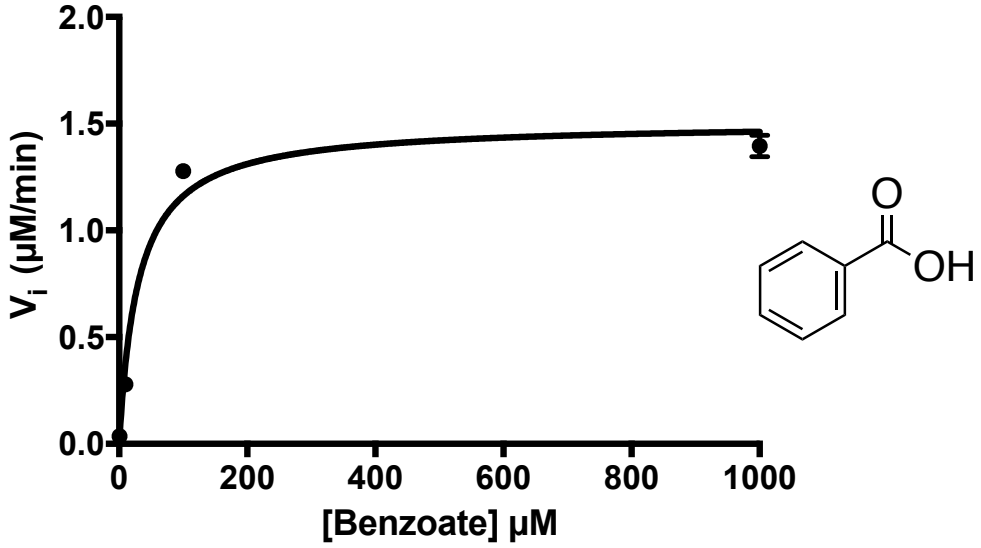
2.0
1.5
1.0
0.5
0.0
V_i (µM/min)
0
200
400
600
800
1000
[Benzoate] µM
O
OH

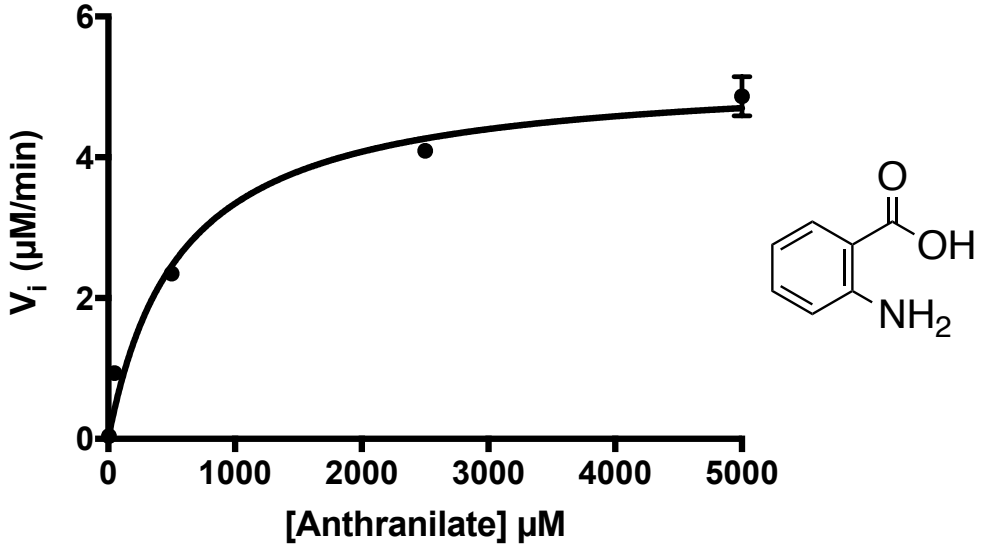
6
4
2
0
V_i (µM/min)
0
1000
2000
3000
4000
5000
[Anthranilate] µM
O
OH
NH_2

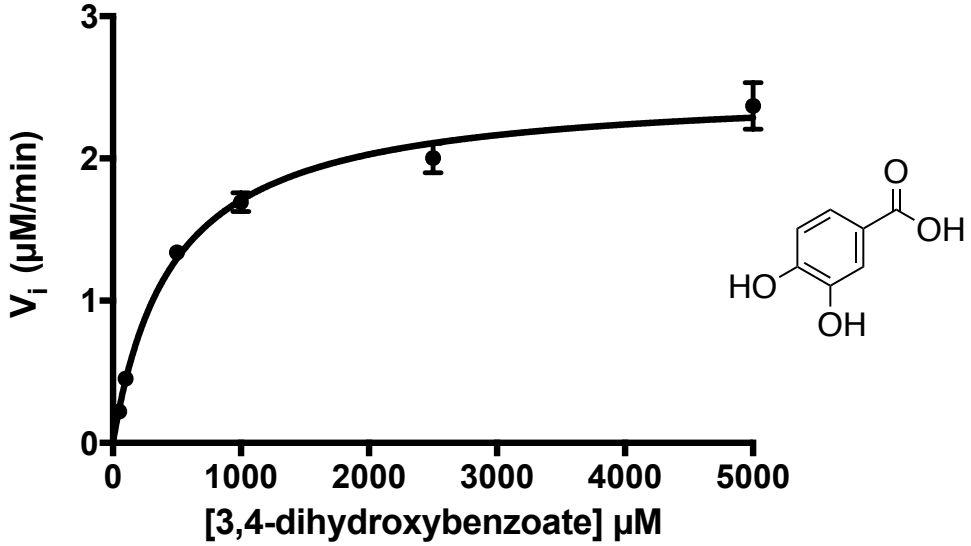
3
2
1
0
V_i (µM/min)
0
1000
2000
3000
4000
5000
[3,4-dihydroxybenzoate] µM
O
OH
HO
OH

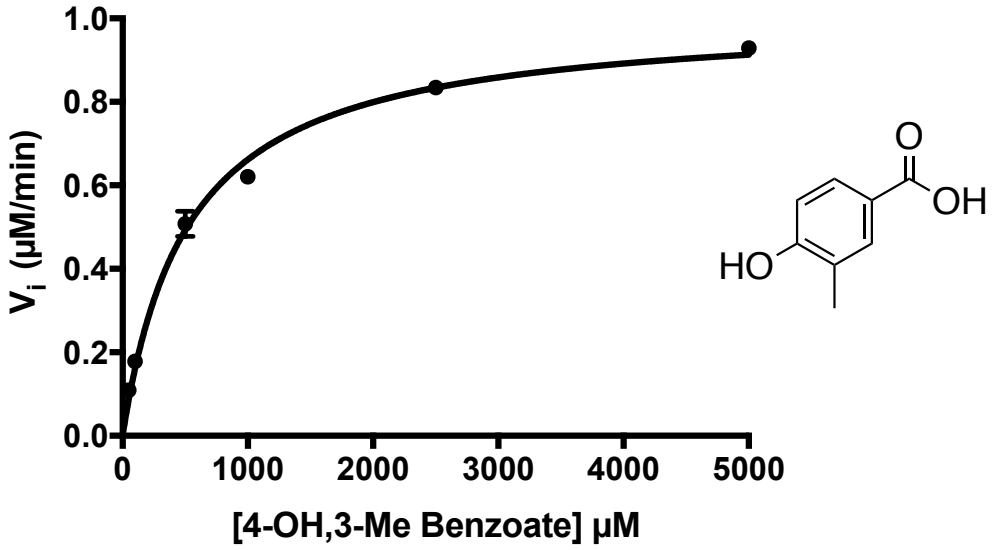
1.0
0.8
0.6
0.4
0.2
0.0
V_i (µM/min)
0
1000
2000
3000
4000
5000
[4-OH,3-Me Benzoate] µM
O
OH
HO

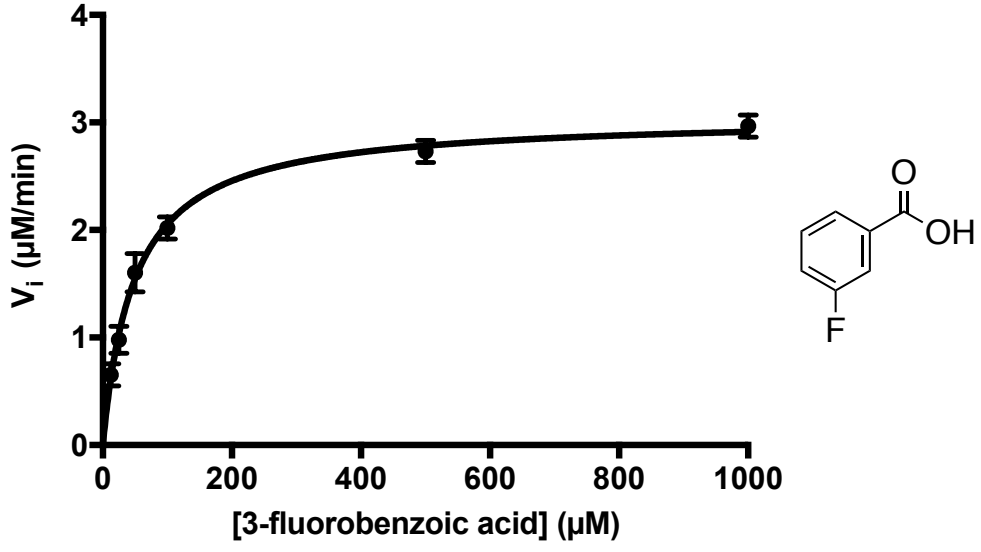
4
3
2
1
0
V_i (µM/min)
0
200
400
600
800
1000
[3-fluorobenzoic acid] (µM)
O
OH
F

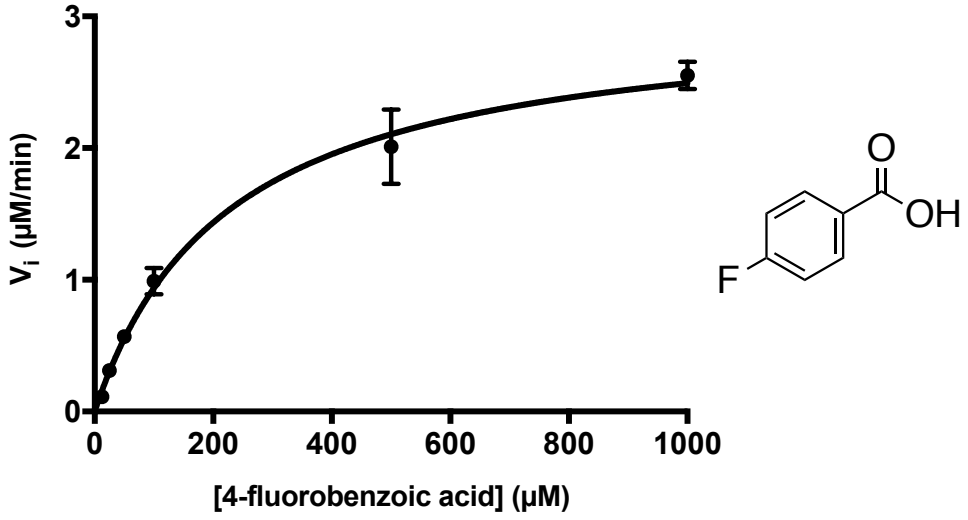
3
2
1
0
V_i (μM/min)
0
200
400
600
800
1000
[4-fluorobenzoic acid] (μM)
O
OH
F

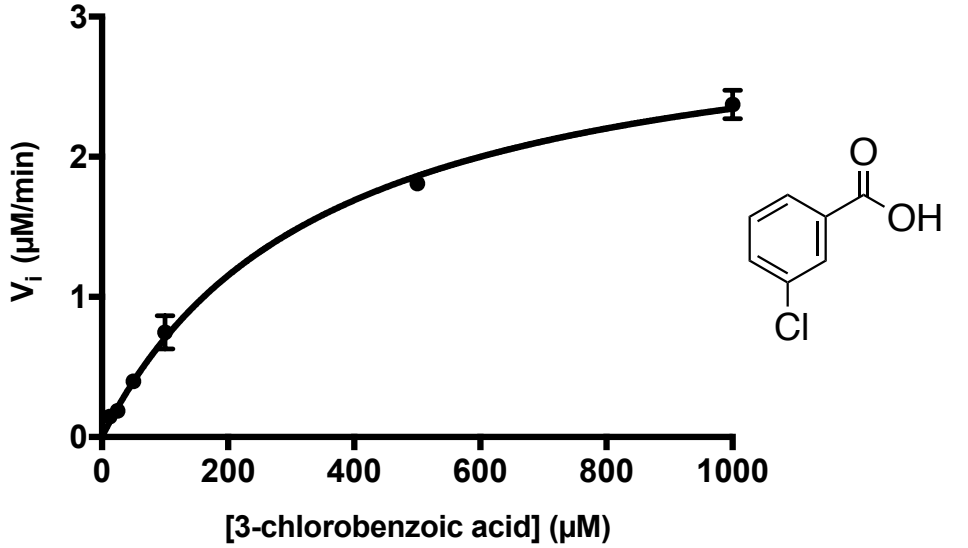
3
2
1
0
V_i (μM/min)
0
200
400
600
800
1000
[3-chlorobenzoic acid] (μM)
O
OH
Cl

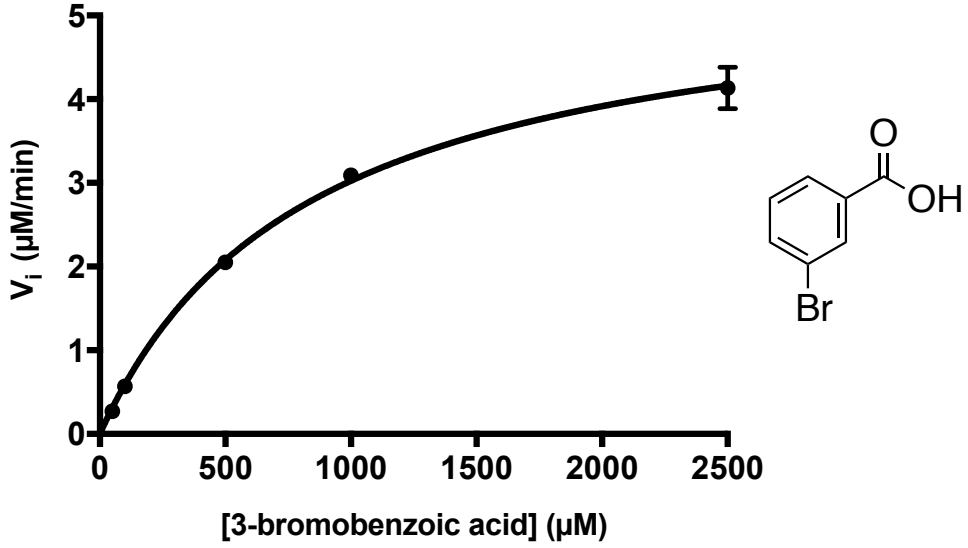
5
4
3
2
1
0
V_i (μM/min)
0
500
1000
1500
2000
2500
[3-bromobenzoic acid] (μM)
O
OH
Br

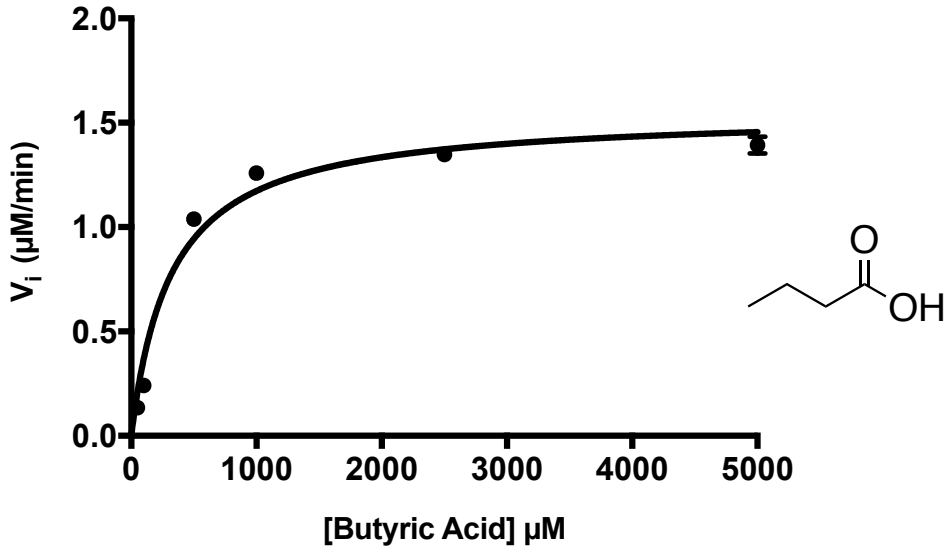

Figure S8. Kinetic analysis of AsuB1$_C$ substrate scope. Initial velocity versus substrate concentration was plotted using the initial velocity values generated using a coupled spectrophotometric assay as described. GraphPad Prism was used to fit a Michaelis-Menten model to generate Vmax and K_m values. Error bars represent standard deviations from at least three independently performed experiments.

A

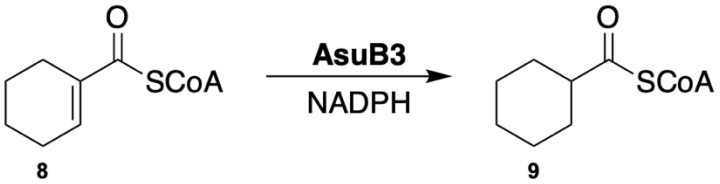

8 9

m/z $[M+H]^+$
Calc. 878.1956
Obs. 878.1950
Error: 0.68 ppm

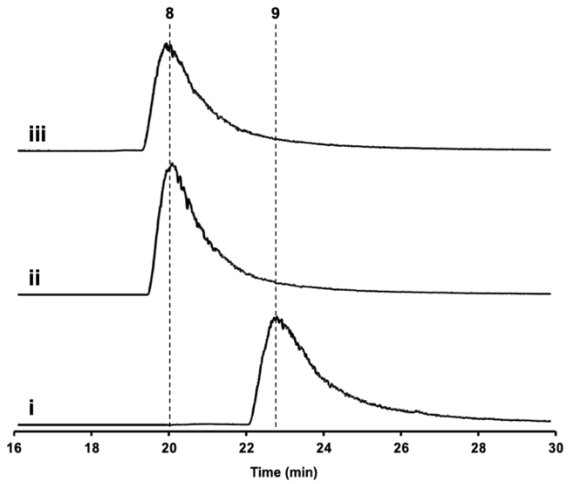

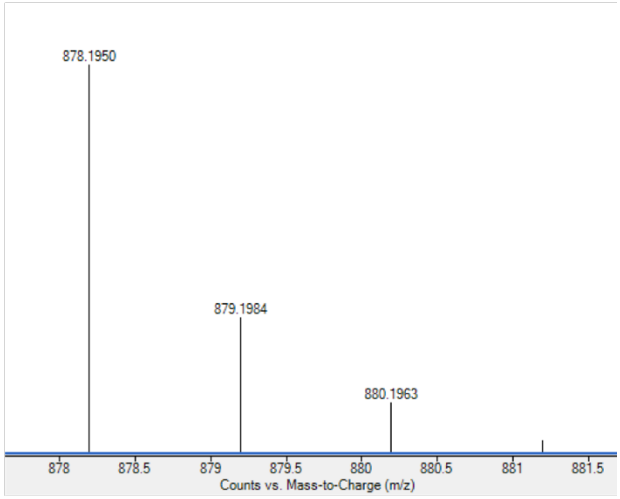

B

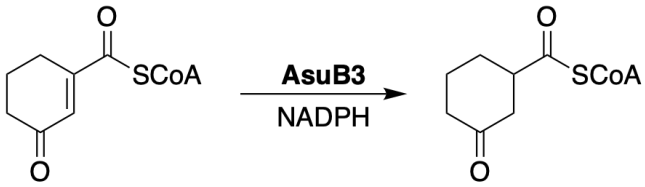

14 15

m/z $[M+H]^+$
Calc. 892.1749
Obs. 892.1735
Error: 1.6 ppm

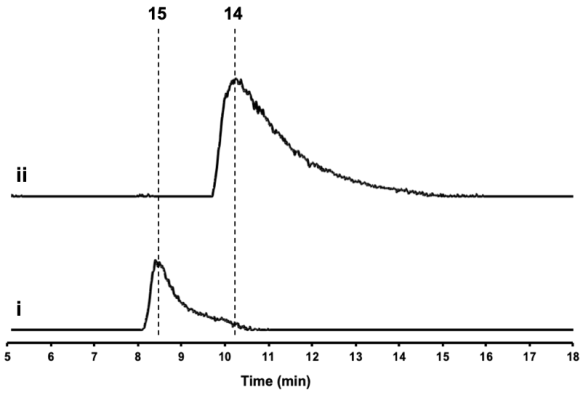

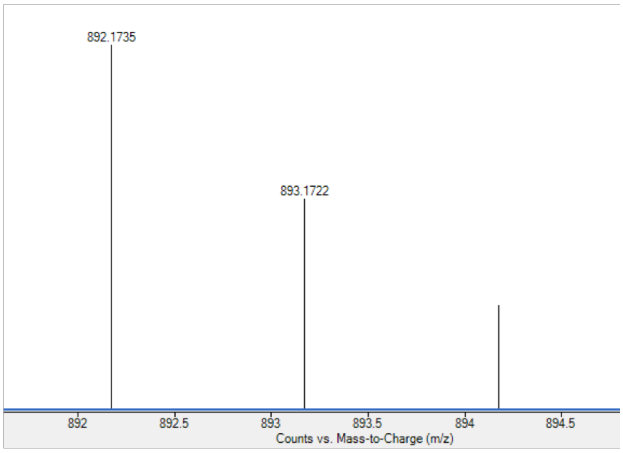

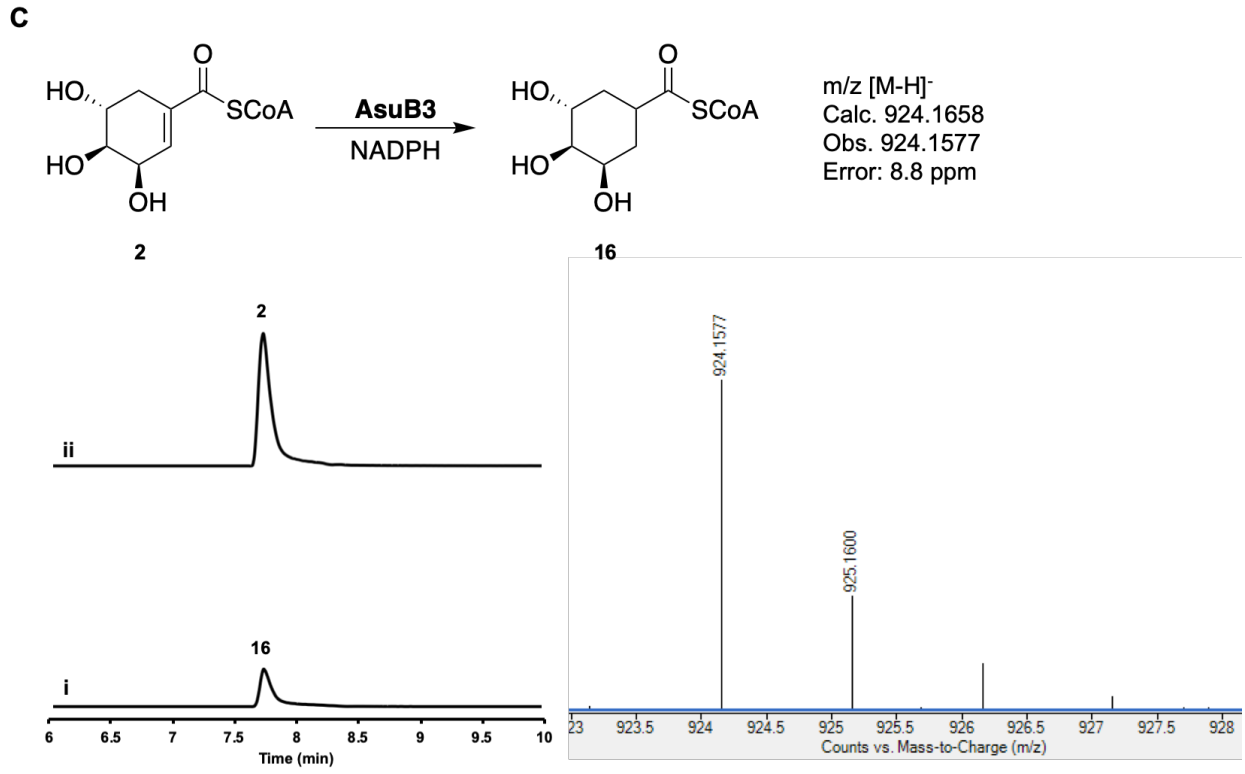

Figure S9. LC-HRMS analysis of AsuB3 catalyzed $\Delta^{1,2}$-reduction. (A) Schematic and HRMS of $\Delta^{1,2}$-reduction of **8**. Extracted ion chromatograms for **8** m/z = 876.1881 $[M+H]^+$ and **9** m/z = 878.1968 $[M+H]^+$ for AsuB3 reaction (trace i), a control lacking AsuB3 (trace ii), and a control lacking NADPH (trace iii). (B) Schematic and HRMS of $\Delta^{1,2}$-reduction of **14.** Extracted ion chromatograms of **14** m/z = 890.1593 $[M+H]^+$ and **15** m/z = 892.1749 for AsuB3 reaction (trace i) and a control lacking AsuB3 (trace ii). (C) Schematic and HRMS of $\Delta^{1,2}$-reduction of **2**. Extracted ion chromatograms of **2** m/z = 922.1502 $[M-H]^-$ and **16** m/z = 924.1658 $[M-H]^-$ for AsuB3 reaction (trace i) and a control lacking AsuB3 (trace ii). The calculated mass with a 10 ppm error tolerance was used.

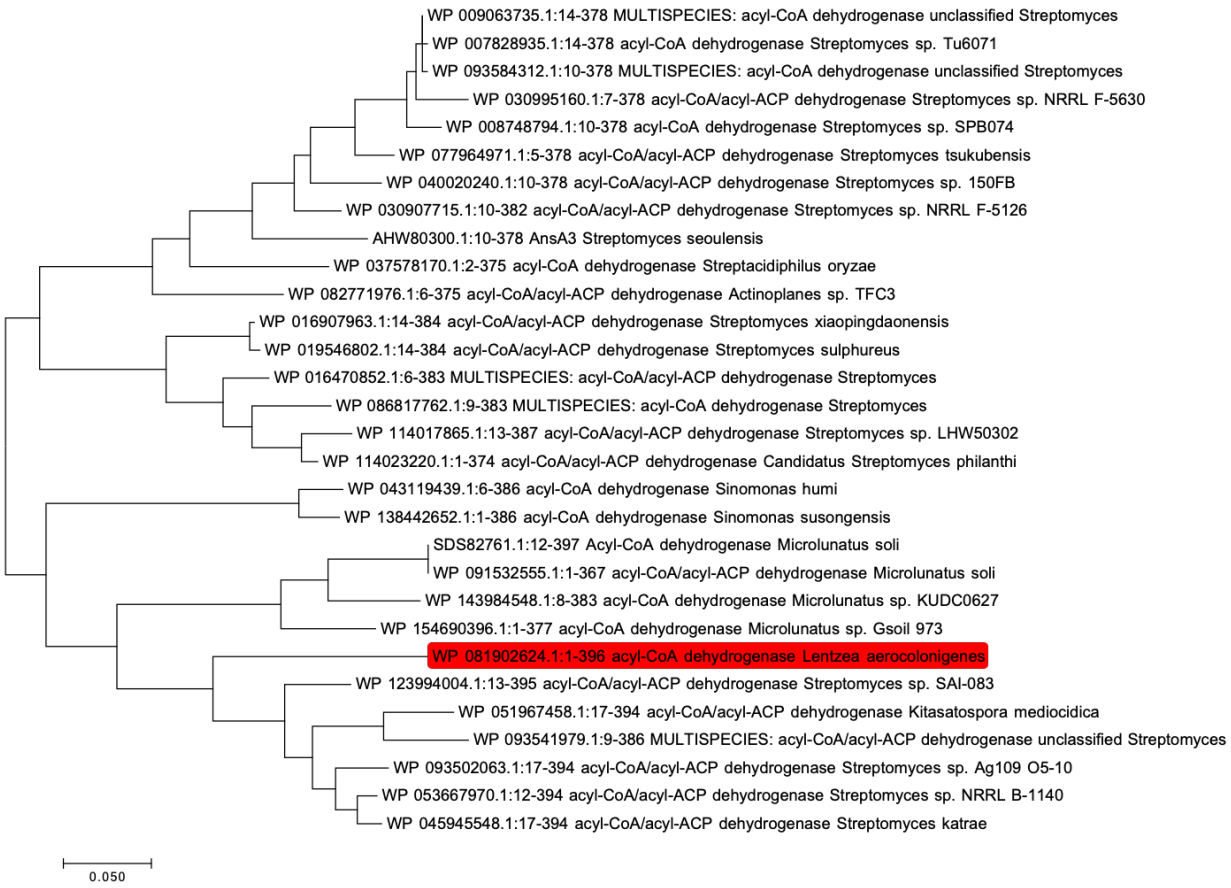

Figure S10. Phylogenetic analysis of AsuB2 (highlighted in red) compared to the top 30 BlastP results. Molecular Phylogenetic analysis by Maximum Likelihood method. The evolutionary history was inferred by using the Maximum Likelihood method based on the JTT matrix-based model.[15] The tree with the highest log likelihood (-5181.48) is shown. Initial tree(s) for the heuristic search were obtained automatically by applying Neighbor-Join and BioNJ algorithms to a matrix of pairwise distances estimated using a JTT model, and then selecting the topology with superior log likelihood value. The tree is drawn to scale, with branch lengths measured in the number of substitutions per site. The analysis involved 30 amino acid sequences. All positions containing gaps and missing data were eliminated. There were a total of 362 positions in the final dataset. Evolutionary analyses were conducted in MEGA7.[16]

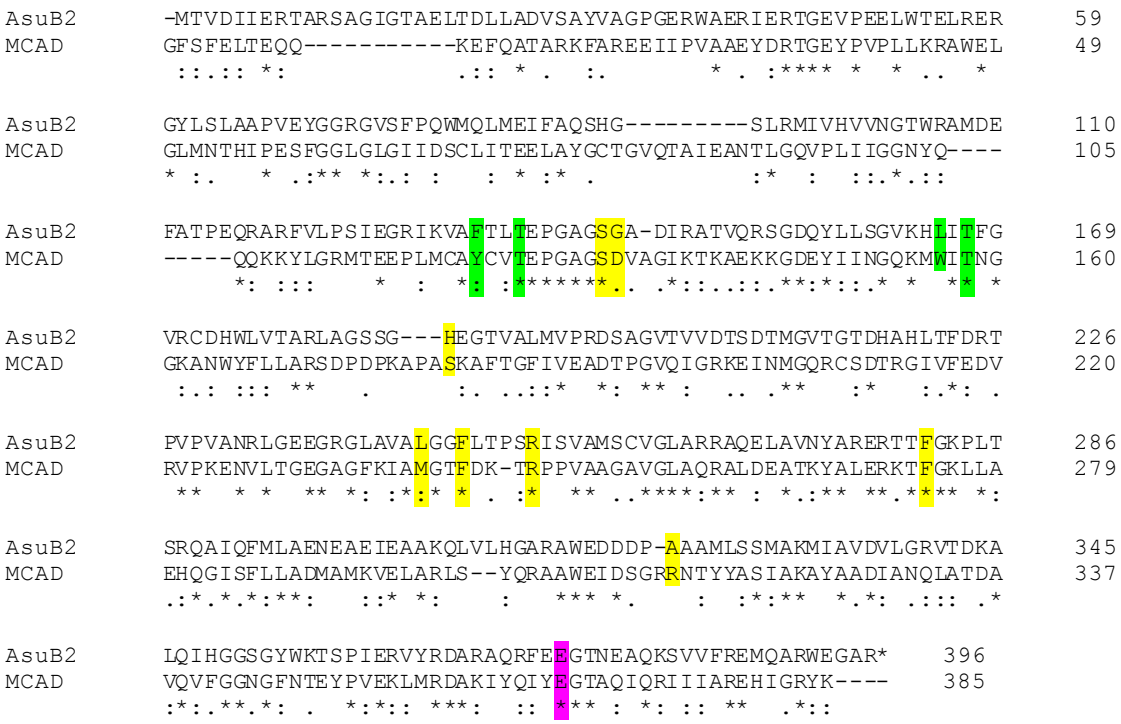

Figure S11. Clustal omega multiple sequence alignment between AsuB2 and pig liver medium chain acyl-CoA dehydrogenase (MCAD). Relevant residues are highlighted according to their involvement in the FAD binding pocket (green), the CoA binding pocket (yellow), and catalysis (purple). The majority of the indicated residues are conserved in AsuB2, including Glu373, which is proposed to remove the α-proton during dehydrogenation.[17]

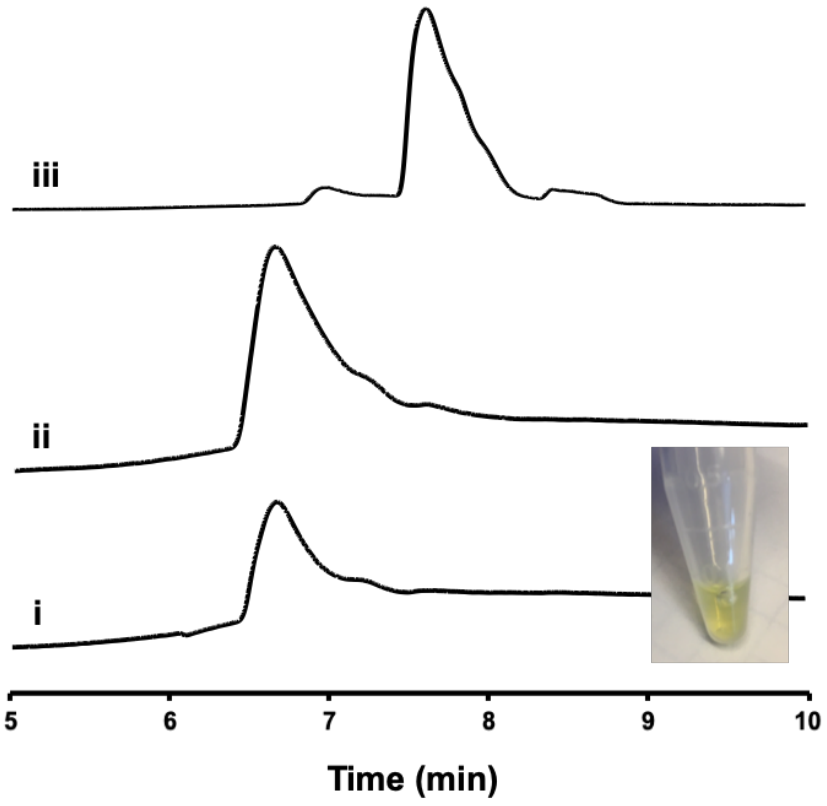

Figure S12. Characterization of AsuB2 as a FAD containing enzyme. LC-UV analysis of an AsuB2 boiled enzyme supernatant (trace i) compared to authentic standards of FAD (ii) and FMN (iii). Purified AsuB2 is shown to exhibit observed yellow color upon purification. UV analysis was monitored at 450 nm. Photo by W. Skyrud.

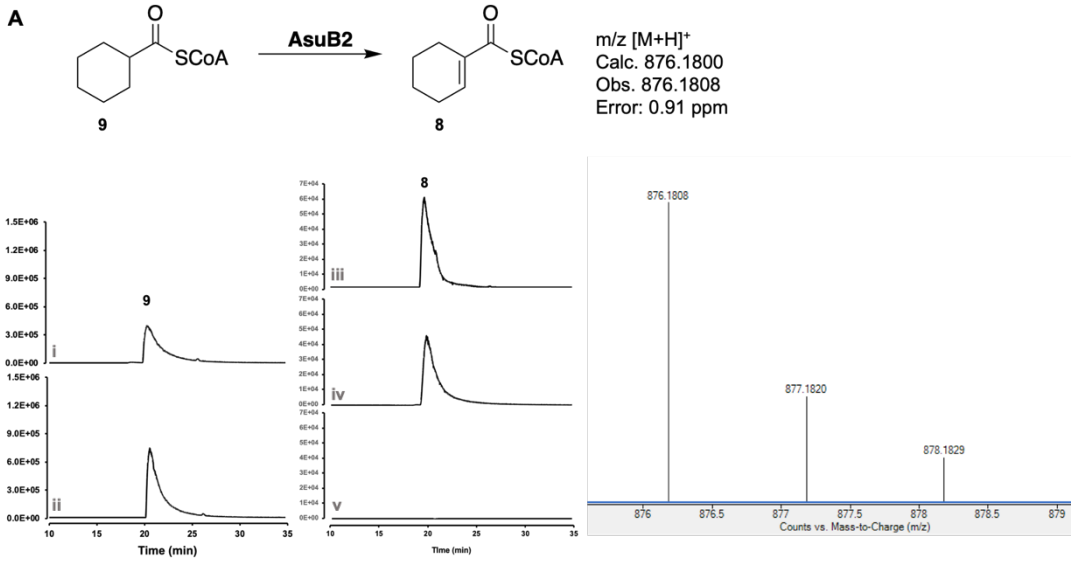
A
O
SCoA
AsuB2
9
8
m/z [M+H]+
Calc. 876.1800
Obs. 876.1808
Error: 0.91 ppm
876.1808
877.1820
878.1829
Counts vs. Mass-to-Charge (m/z)
Time (min)

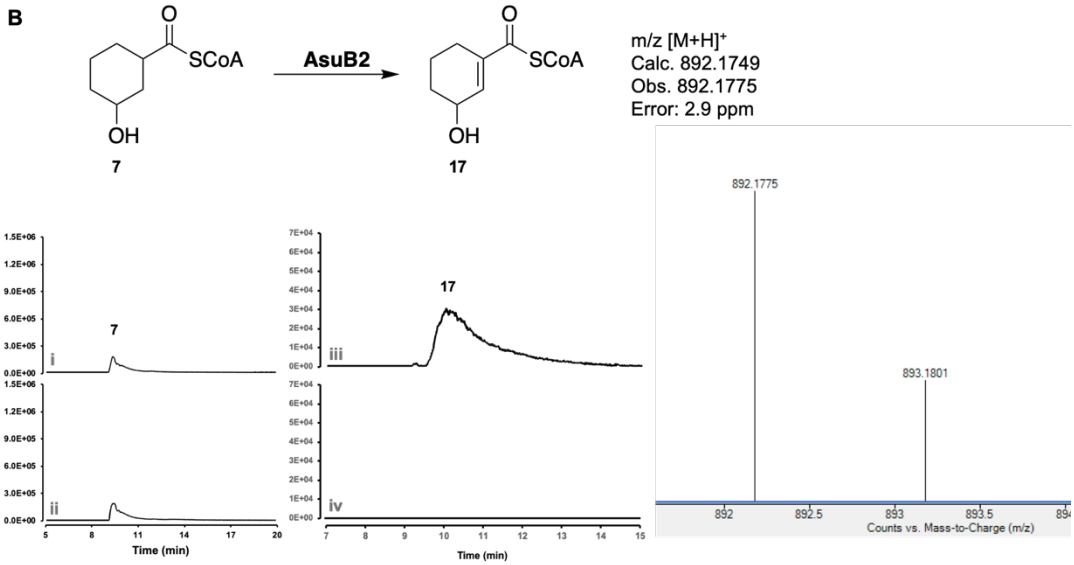
B
O
SCoA
OH
AsuB2
7
17
m/z [M+H]+
Calc. 892.1749
Obs. 892.1775
Error: 2.9 ppm
892.1775
893.1801
Counts vs. Mass-to-Charge (m/z)
Time (min)

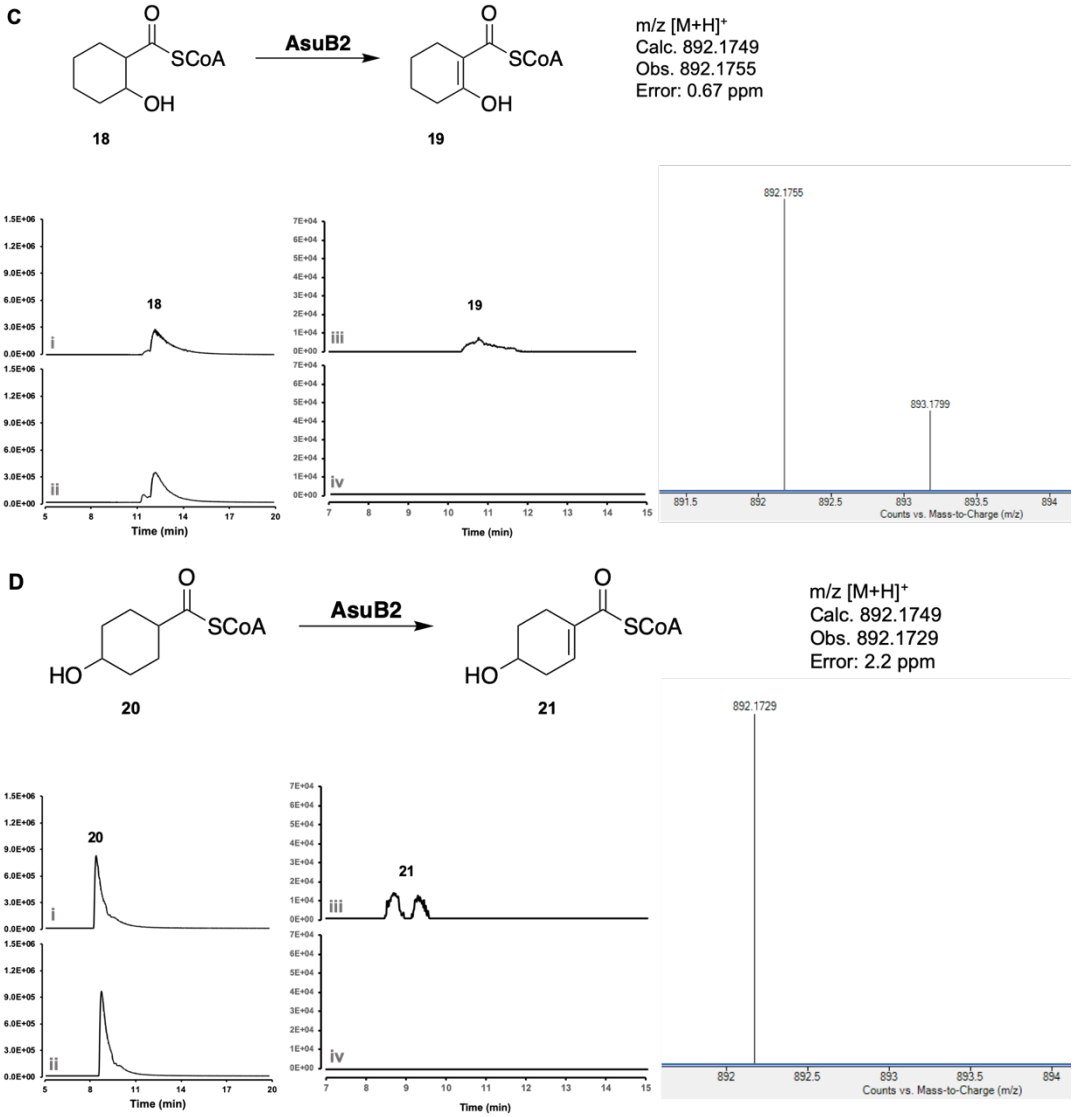

Figure S13. Characterization of AsuB2 dehydrogenase activity. (A) LC-HRMS analysis of dehydrogenation of **9** by AsuB2. Extracted ion chromatograms of **9** m/z = 878.1956 $[M+H]^+$ for AsuB2 reaction (trace i), and a control lacking AsuB2 (trace ii). Extracted ion chromatograms of **8** m/z = 876.1800 $[M+H]^+$ for AsuB2 reaction (trace iv), an enzymatically produced standard of **8** (trace iii), and a control lacking AsuB2 (trace v). (B) LC-HRMS analysis of dehydrogenation of **7** by AsuB2. Extracted ion chromatograms of **7** m/z = 894.1916 $[M+H]^+$ for AsuB2 reaction (trace i) and a control lacking AsuB2 (trace ii). Extracted ion chromatograms of **17** m/z = 892.1749 $[M+H]^+$ for AsuB2 reaction (trace iii) and a control lacking AsuB2 (trace iv). (C) LC-HRMS analysis of dehydrogenation of **18** by AsuB2. Extracted ion chromatograms of **18** m/z = 894.1916 $[M+H]^+$ for AsuB2 reaction (trace i) and a control lacking AsuB2 (trace ii). Extracted ion chromatograms of **19** m/z = 892.1749 $[M+H]^+$ for AsuB2 reaction (trace iii) and a control lacking AsuB2 (trace iv). (D) LC-HRMS analysis of dehydrogenation of **20** by AsuB2. Extracted ion chromatograms of **20** m/z = 894.1916 $[M+H]^+$ for AsuB2 reaction (trace i) and a control lacking AsuB2 (trace ii). Extracted ion chromatograms of **21** m/z = 892.1749 $[M+H]^+$ for AsuB2 reaction (trace iii) and a control lacking AsuB2 (trace iv). The calculated mass with a 10 ppm error tolerance was used.

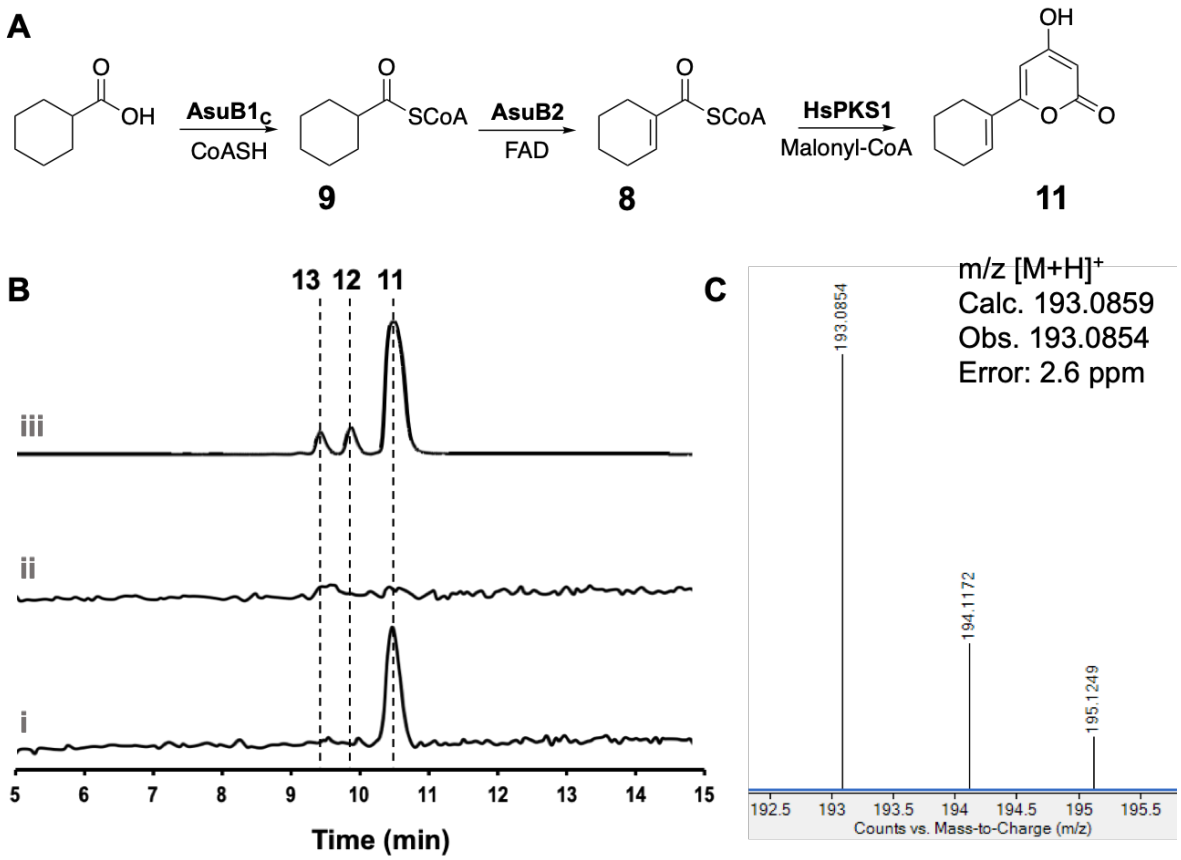

Figure S14. Characterization of the regiospecificity of AsuB2 catalyzed dehydrogenation of **9**. (A) Schematic of the AsuB1$_C$, AsuB2, and HsPKS1 coupled assay. (B) Extracted ion chromatograms of **11** m/z 193.0859 $[M+H]^+$ for coupled reaction (trace i), a control lacking AsuB2 (trace ii), and a standard of **11**, **12** and **13** (trace iii). The calculated mass with a 10 ppm error tolerance was used. (C) LC-HRMS analysis of **11** from trace i.

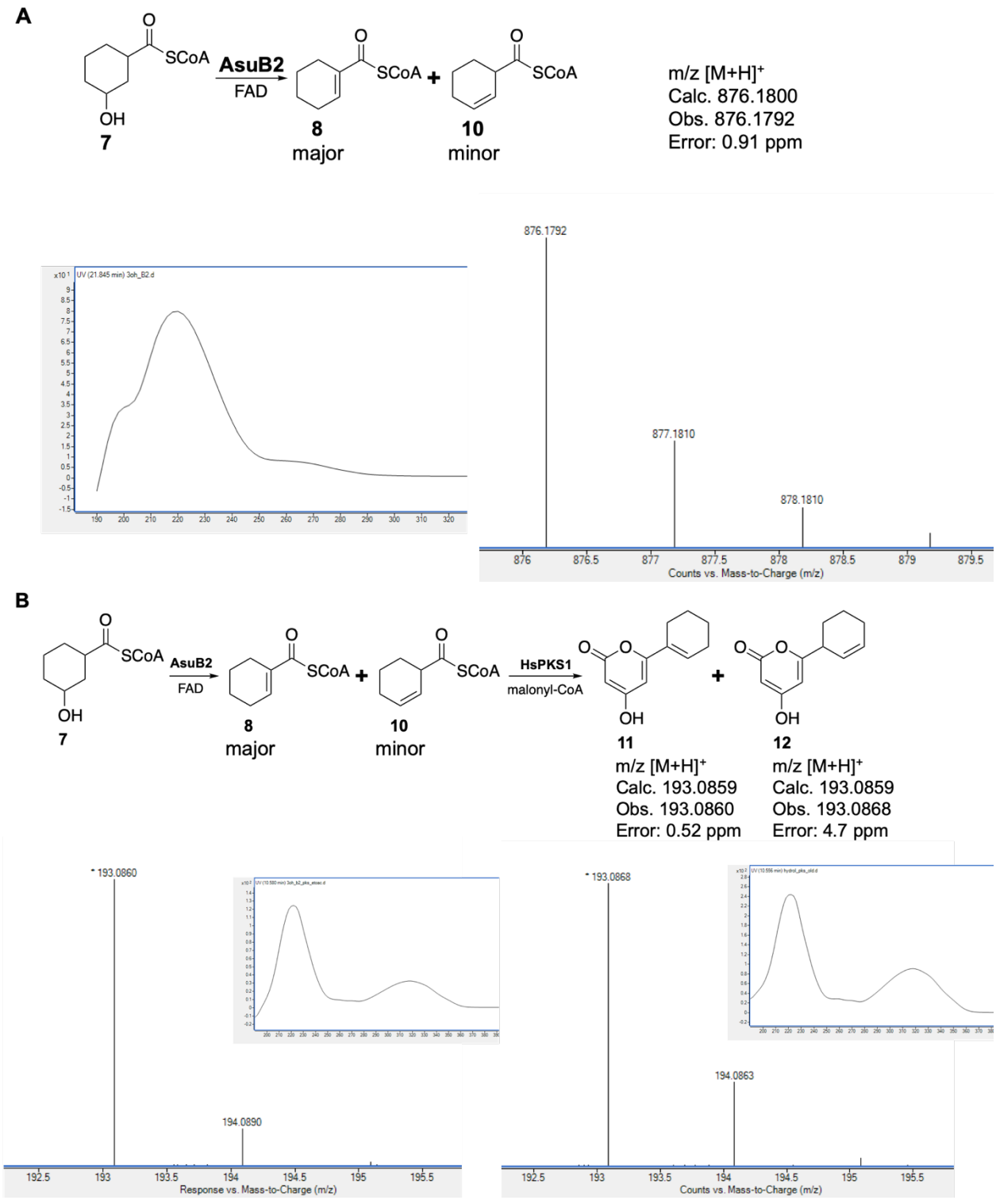

Figure S15. LC-UV-HRMS analysis of dehydration of **7** by AsuB2. (A) Compound characterization of **8** and **10**. (B) compound characterization of **11** and **12**.

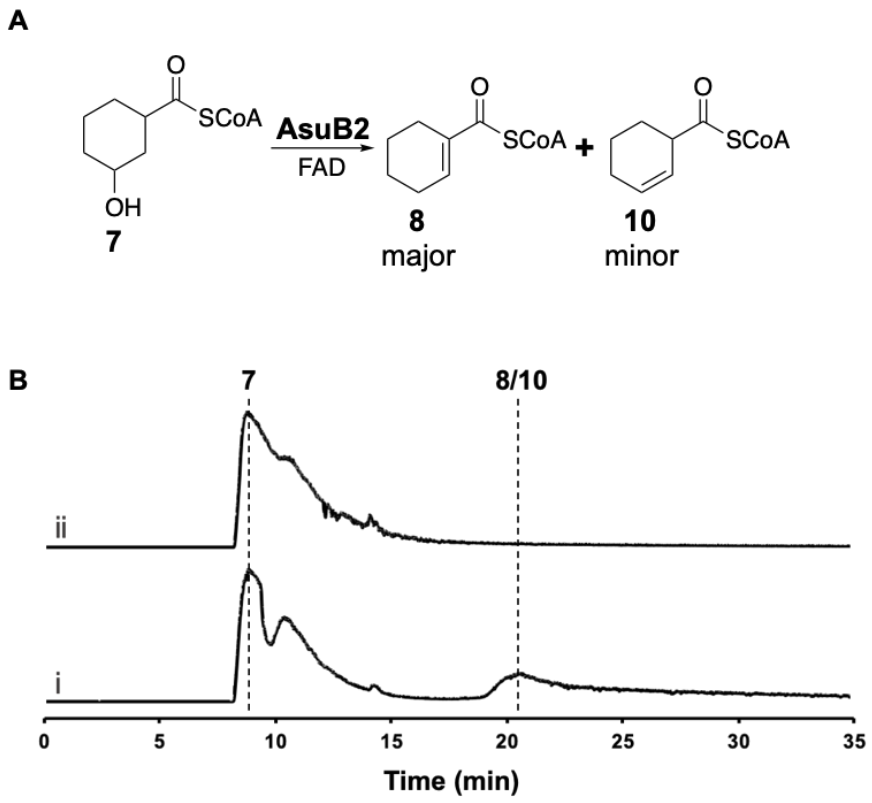

Figure S16. Verification of the FAD dependence of AsuB2 catalyzed dehydration. (A) Schematic of dehydration of **7** to produce **8/10**. (B) Extracted ion chromatograms for **7** m/z = 894.1916 $[M+H]^+$ and **8/10** m/z = 876.1881 $[M+H]^+$ in an AsuB2 reaction (trace i), and a control lacking FAD (trace ii). The calculated mass with a 10 ppm error tolerance was used.

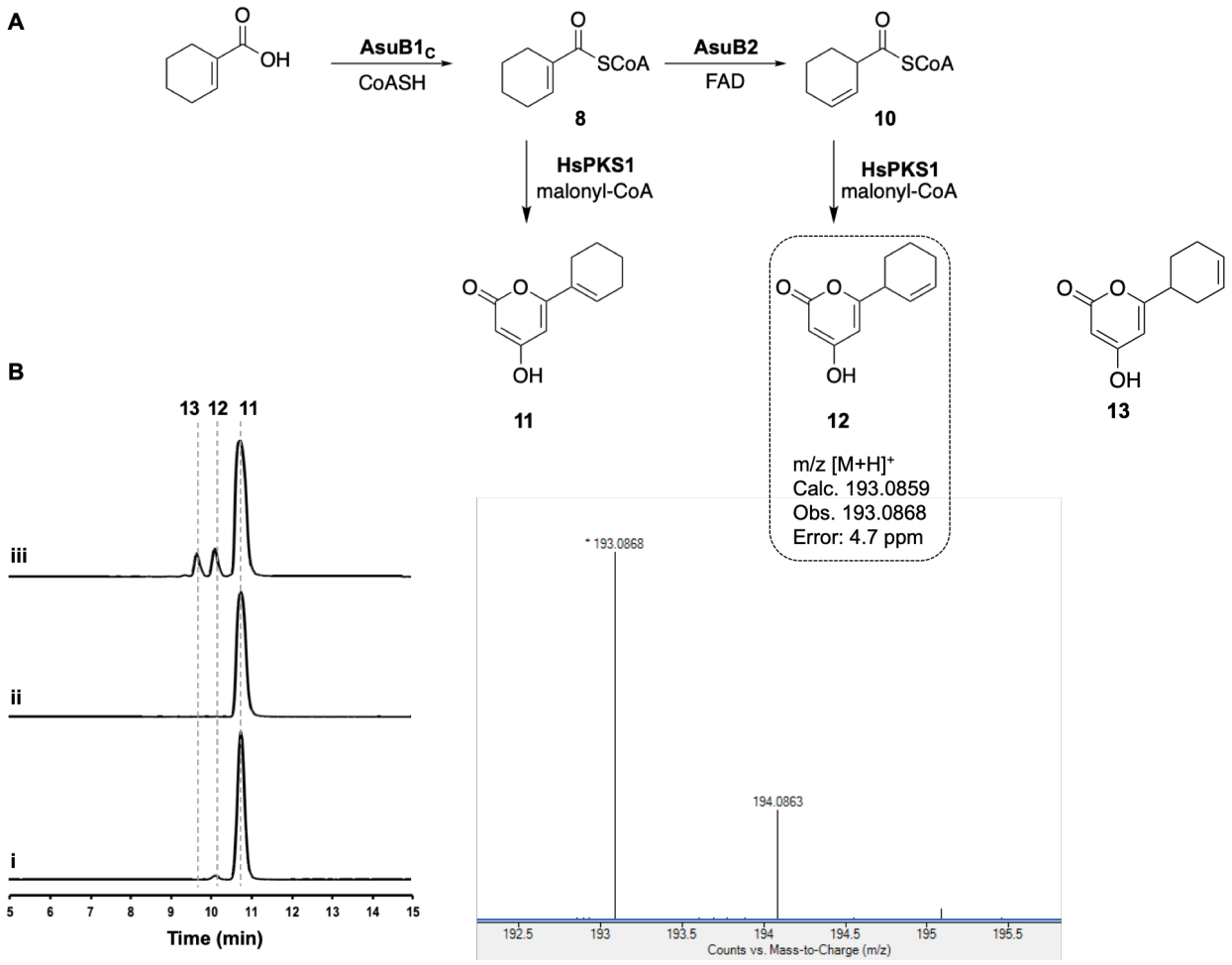

Figure S17. Characterization of AsuB2 isomerase activity. (A) Schematic of coupled AsuB1$_C$, AsuB2, and HsPKS1 coupled assay. (B) Extracted ion chromatograms of **11** and **12** m/z 193.0859 $[M+H]^+$ for coupled reaction (trace i), a control lacking AsuB2 (trace ii), and a standard of **11**, **12** and **13** (trace iii). The calculated mass with a 10 ppm error tolerance was used.

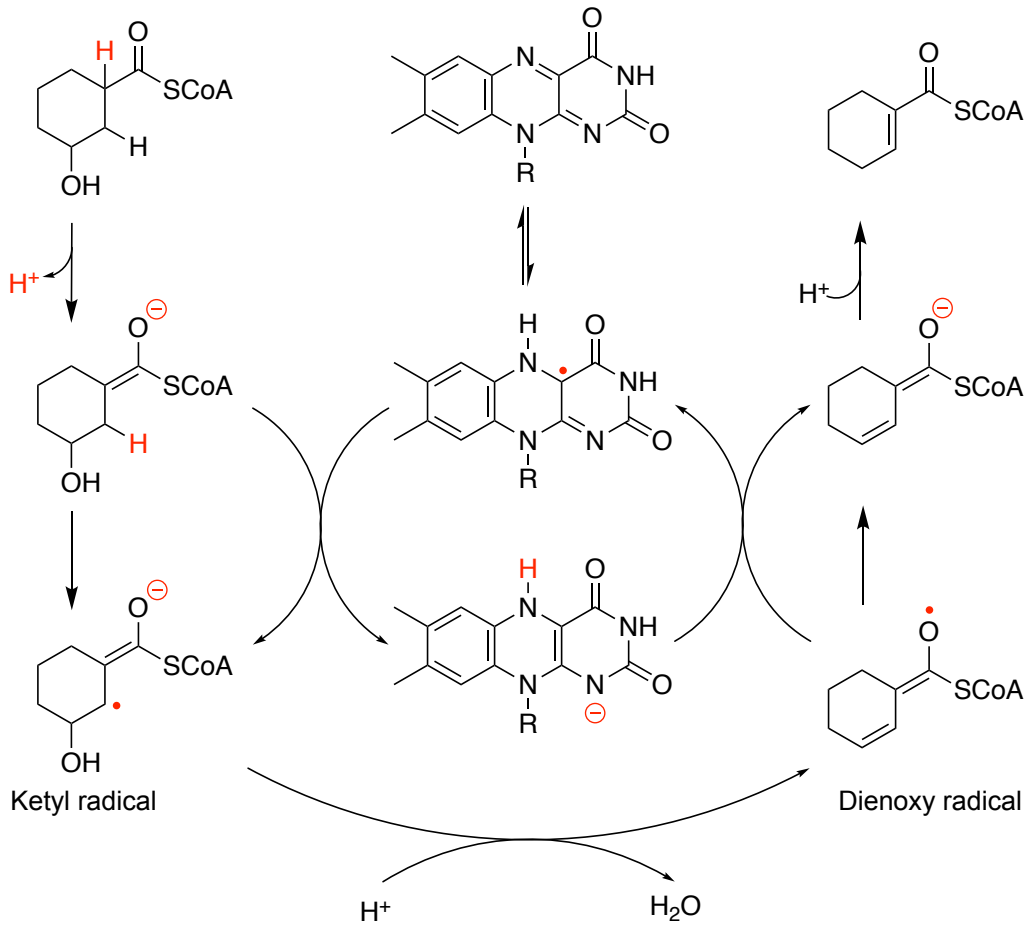

Figure S18. Proposed mechanism for the FAD dependent dehydration of 3-hydroxycyclohexanecarboxyl-CoA by AsuB2.[18]

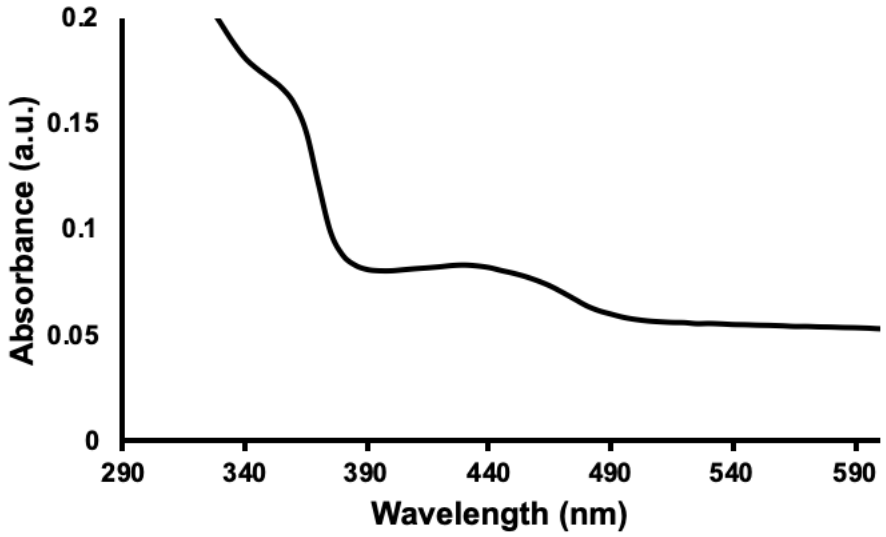

Figure S19. UV-vis analysis of purified AsuB2. A peak at 350 nm and 450 nm is indicative of a low concentration of bound FAD. An obvious peak around 415 nm, indicative of an active iron-sulfur cluster, was not observed.

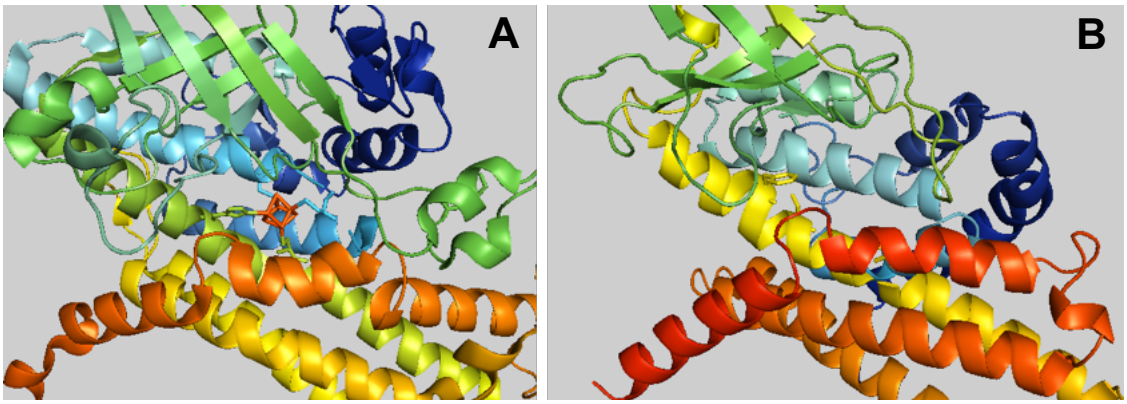

C

```
4-BUDH      MLMTAEQYIESLRKLNTRVYMFGEKIENWVDHPMIRPSINCVRMTYELAQDPQYADLMTT    60
AsuB2       --MTVDI------------------IE----RTARSAGIGT----------AELTDLLAD    26
              **.:                   **    :     .*.           : :**::

4-BUDH      KSNLIGKTINRFANLHQSTDD----LRKKVKMQRLL--------GQKTASCFQRCVGMDA    108
AsuB2       VSAYVAGPGERWAERIERTGEVPEELWTELRERGYLSLAAPVEYGGRGVSFPQWMQLMEI    86
             *  :.   :*:*:  : *.:    * .::: :  *        * : .*  *    *:

4-BUDH      FN----------AVFSTTYEIDQKYGTNYHKNFTEYLKYIQENDLIVDGAMTDPKGDRGL    158
AsuB2       FAQSHGSLRMIVHVVNGTWRAMDEFATPEQR--ARFVLPSIEGRIKVAFTLTEPGAGSGA    144
            *           *.. *:.  :::.*  ::  :.::    *. : *  ::*:* .. *

4-BUDH      APSAQKDPDLFLRIVEKREDGIVVRGAKAHQTGSINSHEHIIMPTIAMTEADKDYAVSFA    218
AsuB2       DIR---------ATVQRSGDQYLLSGVKHLITFGVRCDHWLVTARL-AGSSGHEGTVALM    194
                         *::  *  :: *.*   * .:.... ::   :   .:.:: :*::

4-BUDH      CPSDADGLFMIYGRQSCDTRKMEEGADIDLGNKQFGGQEALVVFDNVFIPNDRIFLCQEY    278
AsuB2       VPRDSAGVTVVDTSDTMG---------------VTGTDHAHLTFDRTPVPVANRLGE---    236
             * *: *: ::   :: .                 * :.* :.**.. :*  . :

4-BUDH      DFAGMMVERFAGYHRQSYGGCKVGVGDVVIGAAALAADYNGAQKASHVKDKLIEMTHLNE    338
AsuB2       ------------F--EGRGLAVALG-----------------------GFLTPSRISV    256
                          .  *  *.:*                        ::  :::.

4-BUDH      TLYCCGIACSAEGYPTA----AGNY--------QIDLLLANVCKQNIT---RFPYEIVRL    383
AsuB2       AMSCVGLARRAQELAVNYARERTTFGKPLTSRQAIQFMLAENE-AEIEAAKQLVLHGARA    315
            :: * *:*  *:   .       .:         *:::**:    :*    ::  . .*

4-BUDH      --AEDIAGGLMVTMPSEADFKSETVVGRDGETIGD--FCNKFFAAAPTCTTEERMRVLRF    439
AsuB2       WEDDDPAAAMLSSM---AKMIAVDVLGRVTDKALQIHGGSGYWKTSPIERVYRDARAQRF    372
               :* *..:: :*   *.: :  *:**  :.  :    . :: ::*   . .  *. **

4-BUDH      LENICLGASAVGYRTESMHGAGSPQAQRIMIARQGNINAKKELAKAIAGIK    490
AsuB2       EEGTNEAQKSVVFREMQARW-------------------------EGAR    396
             *.   . .:* :*  . :                           * :
```

Figure S20. Comparison of the active site of (A) 4-hydroxybutyrl-CoA dehydratase[19] (4-BUDH) and (B) AsuB2. 4-BUDH contains a $[4Fe\text{-}4S]^{2+}$ cluster covalently linked to three Cys (99, 103, 299) residues and one His (292) residue. AsuB2 was modeled using SWISS-MODEL with 1JQI as a template, and shows similar architecture to 4-BUDH. (C) A clustal omega multiple sequence alignment shows no conservation by AsuB2 of the $[4Fe\text{-}4S]^{2+}$ tethering residues (green) or the catalytic residues (yellow) from 4-BUDH.

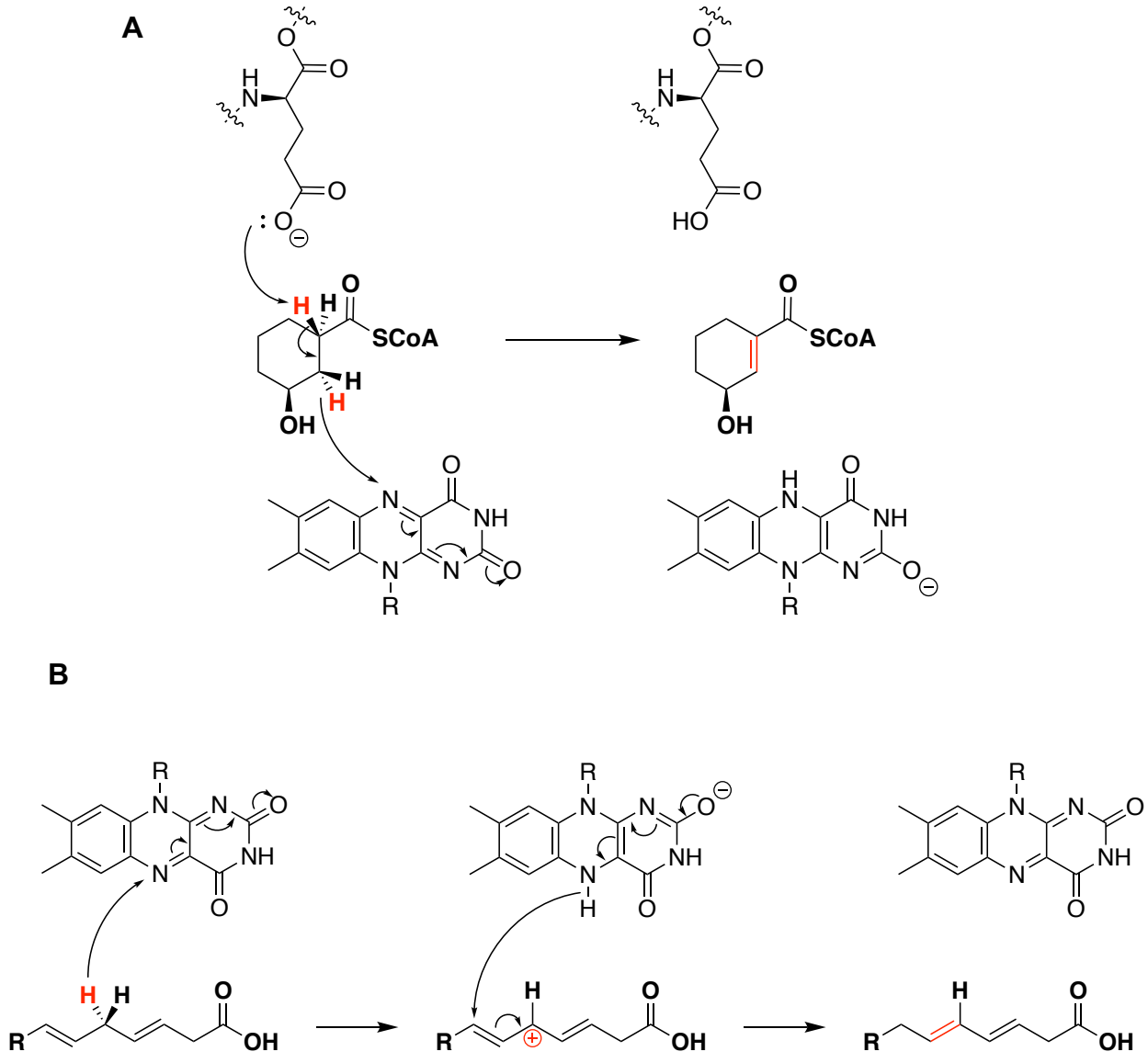

Figure S21. Representative mechanisms of **A** acyl-CoA dehydrogenase and **B** polyunsaturated fatty acid double bond isomerase.[20]

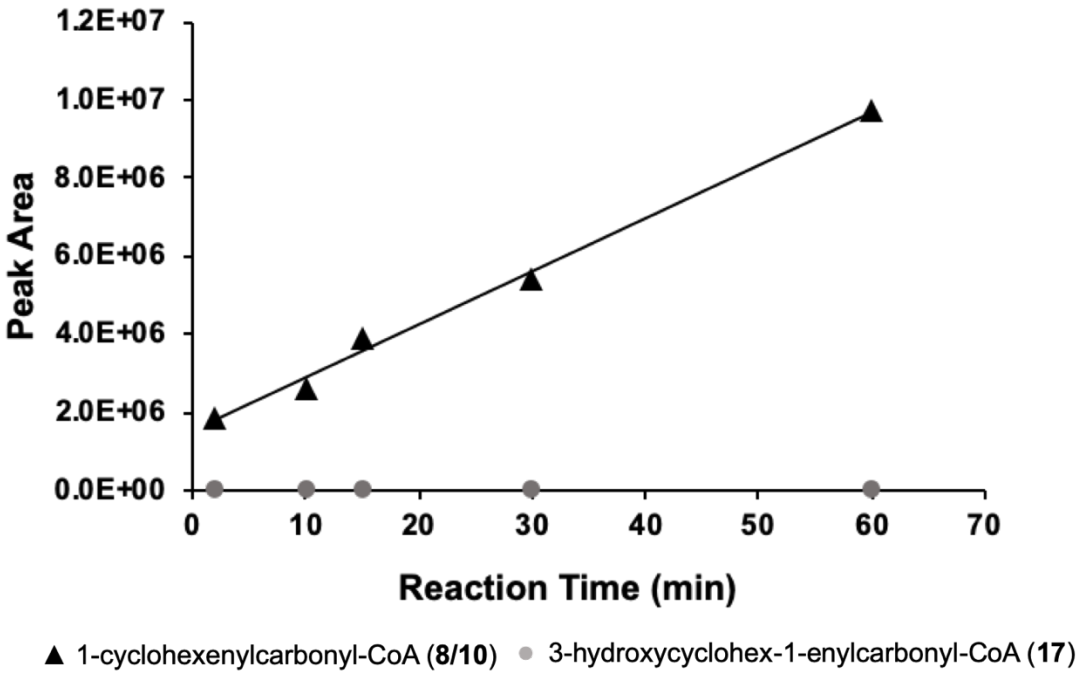

Figure S22. Time course analysis of competing dehydration/dehydrogenation of **7** catalyzed by AsuB2. After 60 minutes there was no presence of the dehydrogenation product (**17**) compared to sufficient production of the dehydration products (**8**/**10**). Formation of the dehydrogenation product required an increase in reaction time to two hours, or an increase in AsuB2 concentration to 20 μM.

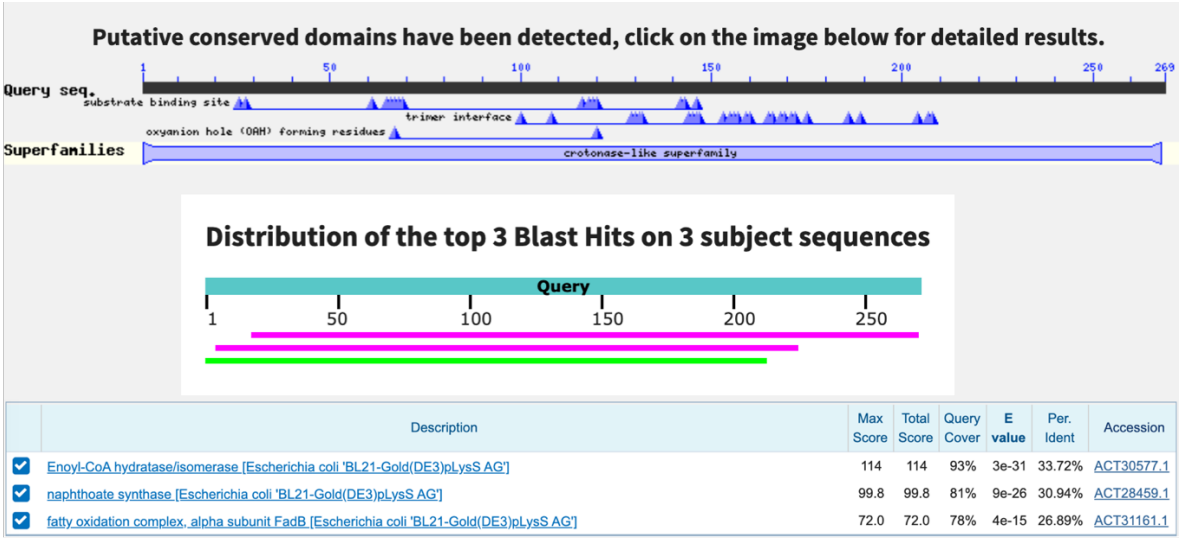

		Description	Max Score	Total Score	Query Cover	E value	Per. Ident	Accession
A	☑	Enoyl-CoA hydratase/isomerase [Escherichia coli 'BL21-Gold(DE3)pLysS AG']	114	114	93%	3e-31	33.72%	ACT30577.1
B	☑	naphthoate synthase [Escherichia coli 'BL21-Gold(DE3)pLysS AG']	99.8	99.8	81%	9e-26	30.94%	ACT28459.1
C	☑	fatty oxidation complex, alpha subunit FadB [Escherichia coli 'BL21-Gold(DE3)pLysS AG']	72.0	72.0	78%	4e-15	26.89%	ACT31161.1

Figure S23. NCBI blastP analysis of *S. collinus* ChcB[21] queried against *E. coli* BL21 Gold. (A) This enoyl-CoA hydratase/isomerase is identical in sequence to CaiD, a well characterized dehydratase.[22] (B) Naphthoate synthase is identical in sequence to MenB, a 1,4-dihydroxy-2-naphthoyl-CoA synthase which is known to catalyze a cyclization reaction in *E. coli* menaquinone biosynthesis.[23] (C) This is the dedicated isomerase of the primary fatty acid oxidation complex in *E. coli.*

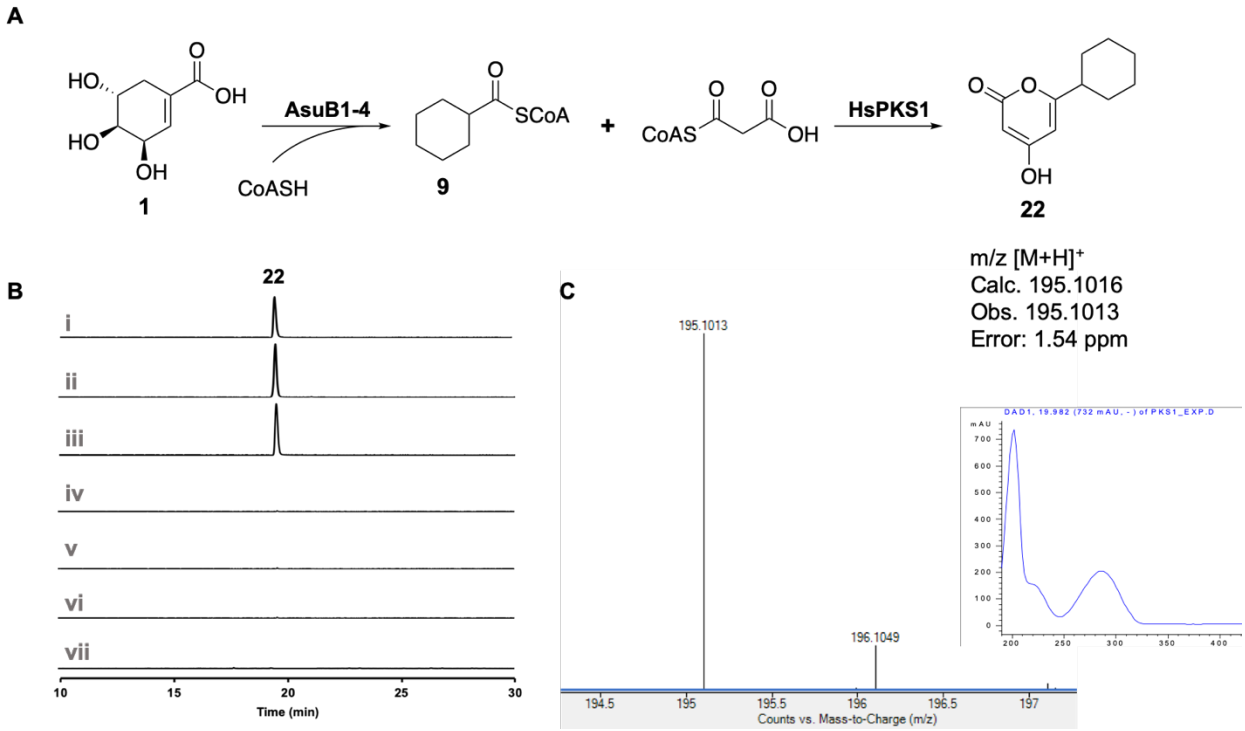

Figure S24. Heterologous production of cyclohexanecarboxyl-CoA in *E. coli.* (A) Schematic of conversion of **1** to **9** catalyzed by AsuB1-4 coupled with HsPKS1 to produce **22**. (B) Extracted ion chromatograms for **22** m/z 195.1016 $[M+H]^+$ for the enzymatically produced standard (trace i), the heterologous production host containing AsuB1-4 and HsPKS1 (trace ii), the heterologous production host containing AsuB1-4, ChcB, and HsPKS1 (trace iii) and control strains lacking, AsuB1 (trace iv), AsuB2 (trace v), AsuB3 (trace vi), and AsuB4 (trace vii). The calculated mass with a 10 ppm error tolerance was used. (C) LC-UV-HRMS analysis of **22** from trace ii.

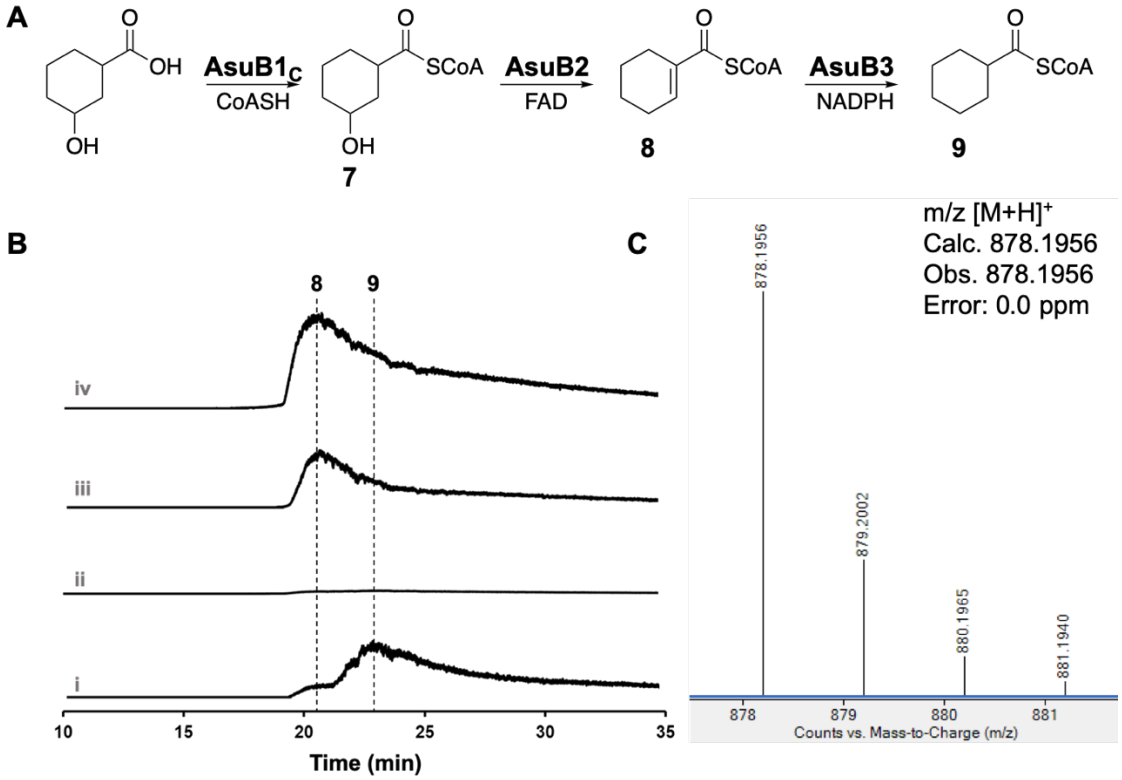

Figure S25. In vitro verification of the proposed final steps of CHC-CoA biosynthesis. (A) Schematic of the AsuB1$_C$, AsuB2, and AsuB3 coupled assay to produce **9**. (B) Extracted ion chromatograms for **9** m/z 878.1956 $[M+H]^+$ for the coupled reaction (trace i) and a control lacking AsuB3 (trace ii), as well as extracted ion chromatograms for **8** m/z = 876.1881 $[M+H]^+$ for the coupled reaction (trace iii) and a control lacking AsuB3 (trace iv). The product of AsuB2 catalyzed dehydration, **8**, is seen in both the coupled reaction and the control lacking AsuB3. Addition of AsuB3 to the coupled reaction generates **9** and leads to a decrease in **8**. The calculated mass with a 10 ppm error tolerance was used. (C) LC-HRMS analysis of **9** from trace i.

References

(1) Rui, Z.; Petrícková, K.; Skanta, F.; Pospísil, S.; Yang, Y.; Chen, C.-Y.; Tsai, S.-F.; Floss, H. G.; Petrícek, M.; Yu, T.-W. Biochemical and Genetic Insights into Asukamycin Biosynthesis. *J. Biol. Chem.* **2010**, *285* (32), 24915–24924.

(2) Labeda, D. P.; Kroppenstedt, R. M. Proposal for the New Genus Allokutzneria Gen. Nov. within the Suborder Pseudonocardineae and Transfer of Kibdelosporangium Albatum Tomita et Al. 1993 as Allokutzneria Albata Comb. Nov. *Int. J. Syst. Evol. Microbiol.* **2008**, *58* (Pt 6), 1472–1475.

(3) Labeda, D. P.; Hatano, K.; Kroppenstedt, R. M.; Tamura, T. Revival of the Genus Lentzea and Proposal for Lechevalieria Gen. Nov. *Int. J. Syst. Evol. Microbiol.* **2001**, *51* (Pt 3), 1045–1050.

(4) Zhao, X.; Geng, X.; Chen, C.; Chen, L.; Jiao, W.; Yang, C. Draft Genome Sequence of the Marine Actinomycete Streptomyces Sulphureus L180, Isolated from Marine Sediment. *J. Bacteriol.* **2012**, *194* (16), 4482.

(5) Chen, S.; von Bamberg, D.; Hale, V.; Breuer, M.; Hardt, B.; Müller, R.; Floss, H. G.; Reynolds, K. A.; Leistner, E. Biosynthesis of Ansatrienin (Mycotrienin) and Naphthomycin. Identification and Analysis of Two Separate Biosynthetic Gene Clusters in Streptomyces Collinus Tü 1892. *Eur. J. Biochem.* **1999**, *261* (1), 98–107.

(6) Sekiyama, Y.; Palaniappan, N.; Reynolds, K. A.; Osada, H. Biosynthesis of Phoslactomycins: Cyclohexanecarboxylic Acid as the Starter Unit. *Tetrahedron* **2003**, *59*, 7465–7471.

(7) Sugita, M.; Natori, Y.; Sasaki, T.; Furihata, K.; Shimazu, A.; Seto, H.; Otake, N. Studies on Mycotrienin Antibiotics, a Novel Class of Ansamycins. I. Taxonomy, Fermentation, Isolation and Properties of Mycotrienins I and II. *J. Antibiot. (Tokyo).* **1982**, *35* (11), 1460–1466.

(8) Cropp, T. A.; Wilson, D. J.; Reynolds, K. A. Identification of a Cyclohexylcarbonyl CoA Biosynthetic Gene Cluster and Application in the Production of Doramectin. *Nat. Biotechnol.* **2000**, *18* (9), 980–983.

(9) Gibson, J.; Dispensa, M.; Fogg, G. C.; Evans, D. T.; Harwood, C. S. 4-Hydroxybenzoate-Coenzyme A Ligase from Rhodopseudomonas Palustris: Purification, Gene Sequence, and Role in Anaerobic Degradation. *J. Bacteriol.* **1994**, *176* (3), 634–641.

(10) Kawaguchi, K.; Shinoda, Y.; Yurimoto, H.; Sakai, Y.; Kato, N. Purification and Characterization of Benzoate-CoA Ligase from Magnetospirillum Sp. Strain TS-6 Capable of Aerobic and Anaerobic Degradation of Aromatic Compounds. *FEMS Microbiol. Lett.* **2006**, *257* (2), 208–213.

(11) Samanta, S. K.; Harwood, C. S. Use of the Rhodopseudomonas Palustris Genome Sequence to Identify a Single Amino Acid That Contributes to the Activity of a Coenzyme A Ligase with Chlorinated Substrates. *Mol. Microbiol.* **2005**, *55* (4), 1151–1159.

(12) Gulick, A. M.; Lu, X.; Dunaway-Mariano, D. Crystal Structure of 4-Chlorobenzoate:CoA Ligase/Synthetase in the Unliganded and Aryl Substrate-Bound Statest. *Biochemistry* **2004**, *43* (27), 8670–8679.

(13) Black, P. N.; DiRusso, C. C.; Metzger, A. K.; Heimert, T. L. Cloning, Sequencing, and Expression of the FadD Gene of Escherichia Coli Encoding Acyl Coenzyme A Synthetase. *J. Biol. Chem.* **1992**, *267* (35), 25513–25520.

(14) Zhang, W.; Bolla, M. L.; Kahne, D.; Walsh, C. T. A Three Enzyme Pathway for 2-Amino-

3-Hydroxycyclopent-2-Enone Formation and Incorporation in Natural Product Biosynthesis. *J. Am. Chem. Soc.* **2010**, *132* (18), 6402–6411.
(15) Jones, D. T.; Taylor, W. R.; Thornton, J. M. The Rapid Generation of Mutation Data Matrices. *Bioinformatics* **1992**, *8* (3), 275–282.
(16) Kumar, S.; Stecher, G.; Tamura, K. MEGA7: Molecular Evolutionary Genetics Analysis Version 7.0 for Bigger Datasets. *Mol. Biol. Evol.* **2016**, *33* (7), 1870–1874.
(17) Kim, J. J. P.; Wang, M.; Paschke, R. Crystal Structures of Medium-Chain Acyl-CoA Dehydrogenase from Pig Liver Mitochondria with and without Substrate. *Proc. Natl. Acad. Sci. U. S. A.* **1993**, *90* (16), 7523–7527.
(18) Zhang, J.; Friedrich, P.; Pierik, A. J.; Martins, B. M.; Buckel, W. Substrate-Induced Radical Formation in 4-Hydroxybutyryl Coenzyme a Dehydratase from Clostridium Aminobutyricum. *Appl. Environ. Microbiol.* **2015**, *81* (3), 1071–1084.
(19) Martins, B. M.; Dobbek, H.; Cinkaya, I.; Buckel, W.; Messerschmidt, A. Crystal Structure of 4-Hydroxybutyryl-CoA Dehydratase: Radical Catalysis Involving a [4Fe-4S] Cluster and Flavin. *Proc. Natl. Acad. Sci.* **2004**, *101* (44), 15645–15649.
(20) Liavonchanka, A.; Rudolph, M. G.; Tittmann, K.; Hamberg, M.; Feussner, I. On the Mechanism of a Polyunsaturated Fatty Acid Double Bond Isomerase from Propionibacterium Acnes. *J. Biol. Chem.* **2009**, *284* (12), 8005–8012.
(21) Patton, S. M.; Cropp, T. A.; Reynolds, K. A. A Novel Δ3,Δ2-Enoyl-CoA Isomerase Involved in the Biosynthesis of the Cyclohexanecarboxylic Acid-Derived Moiety of the Polyketide Ansatrienin A. *Biochemistry* **2000**, *39*, 7595–7604.
(22) Elssner, T.; Engemann, C.; Baumgart, K.; Kleber, H. P. Involvement of Coenzyme a Esters and Two New Enzymes, an Enoyl-CoA Hydratase and a CoA-Transferase, in the Hydration of Crotonobetaine to L-Carnitine by Escherichia Coli. *Biochemistry* **2001**, *40* (37), 11140–11148.
(23) Li, H.-J.; Li, X.; Liu, N.; Zhang, H.; Truglio, J. J.; Mishra, S.; Kisker, C.; Garcia-Diaz, M.; Tonge, P. J. Mechanism of the Intramolecular Claisen Condensation Reaction Catalyzed by MenB, a Crotonase Superfamily Member. *Biochemistry* **2011**, *50* (44), 9532–9544.